

RU-568

Flow Research Report No. 209

**Norton Sound and Bering Sea
Ice Motion: 1981**

b y

D. R. Thomas

and

R. S. Pritchard

October 1981

**Flow Research Company
A Division of Flow Industries, Inc.
21414-68th Avenue South
Kent, Washington 98031
(206) 872-8500**

Annual Report
May 80 - April 81
Research Unit 567 & 568

THE TRANSPORT AND BEHAVIOR OF
OIL SPILLED IN AND UNDER SEA ICE

D. R. Thomas

R. S. Pritchard

Flow Research Company
A Division of Flow Industries, Inc.
21414-68th Avenue South
Kent, Washington 98031
(206) 872-8500

March 31, 1982

TABLE OF CONTENTS

	Page
1. SWRY OF OBJECTIVES, CONCLUSIONS AND IMPLICATIONS	1
11. INTRODUCTION	1
A. General Nature and Scope of Work	1
B. Specific Objectives	2
C. Relevance to Problems of Petroleum Development	2
111. CURRENT STATE OF KNOWLEDGE	2
IV. STUDY AREA	3
v. SOURCES METHODS AND RATIONALE OF DATA COLLECTION	3
VI. RESULTS	4
A. Buoy Deployment	4
B. Modeling Work	5
VII. DISCUSSION AND CONCLUSIONS	6
VIII . NEED FOR FURTHER STUDY	8
Ix. SUMMARY OF OPERATIONS	9
A. Chukchi Sea Buoy Deployment , 16-18 December 1981	9
(1) Buoy Description	9
(2) Logistics	9
(3) Deployment Locations	9
(4) Ice Conditions	10
(5) Remarks	10
(6) Scientific Personnel	10
B. Chukchi Sea Buoy Deployment, 7-16 February 1982	10
(1) Buoy Description	10
(2) Logistics	10
(3) Deployment Locations	11
(4) Ice Conditions	11
(5) Remarks	11
(6) Scientific Personnel	11
C. Chukchi Sea Buoy Retrieval Attempt, 14-17 March 1982	11
(1) Purpose of Trip	11
(2) Logistics	12
(3) Search Location	12
(4) Ice Conditions	12
(5) Results	12
(6) Scientific Personnel	13

TABLE OF CONTENTS

	Page
D. Norton Sound Buoy Deployment, 16-19 December 1981	13
(1) Buoy Description	13
(2) Logistics	13
(3) Deployment Locations	13
(4) Ice Conditions	14
(5) Remarks	14
(6) Scientific Personnel	14
E. Norton Sound Buoy Deployment, 29 January - 5 February 1982	14
(1) Buoy Description	14
(2) Logistics	14
(3) Deployment Locations	14
(4) Ice Conditions	14
(5) Remarks	15
(6) Scientific Personnel	15
F. Norton Sound Buoy Deployment, 23 February - 5 March 1982	15
(1) Buoy Description	15
(2) Logistics	15
(3) Deployment Locations	15
(4) Ice Conditions	15
(5) Remarks	16
(6) Scientific Personnel	17
References	17
Supplementary Material	18
A. Meetings Attended	18
B. Publications	18
Appendix A. Buoy Descriptions	A1
Appendix B. Norton South and Bering Sea Ice Motion: 1981	B1
Appendix C. The Turbulent Boundary Layer in Shallow Water	c1

1. SUMMARY OF OBJECTIVES, CONCLUSIONS AND IMPLICATIONS

During the past year, this research unit has directed its efforts toward understanding the behavior of sea ice in the Beaufort, **Chukchi** and Bering Seas. Environmental data consisting of ice motions, ocean currents and winds or barometric pressure readings have been collected in the Bering and **Chukchi** Seas. In addition, simulations of nearshore ice behavior in the Diapir lease area are being undertaken in order to provide material for developing better winter oil spill trajectories.

The ice drift data for the Bering and **Chukchi** Seas show that extreme ice motion can occur in those areas. In particular, ice motions in and near the Bering Strait can be large, 50 km per day or more, and in a northerly or southerly direction. Ice trajectories have also been observed to lead from Norton Sound to near the Siberian coast.

Ice conditions also vary widely in the Bering and **Chukchi** Seas. Because of the large ice motions, a great deal of open water is produced which quickly becomes thin ice. This thin ice has insignificant compressive strength and is easily deformed during periods of ice convergence.

Oil spills in the Bering and **Chukchi** Seas will be extremely difficult to clean up due to the large ice motions and the amount of thin ice, open water and deformed ice. The presence of a foreign coast nearby, as well as the biologically productive Bering Sea, makes prevention and cleanup of oil spills extremely important.

11. INTRODUCTION

A. General Nature and Scope of Work

The work being performed by this research unit is focused on the interaction of oil spills and sea ice in the Arctic waters off the Alaskan coast. One aim is to synthesize available knowledge about oil and sea ice in order to produce specific oil spill scenarios. An especially important aspect of oil and ice interaction is the transport of oil by the ice cover. Oil spilled on or beneath sea ice will be incorporated in the moving ice cover until spring, when it will emerge from the melting ice to begin harmful interactions with the environment. Thus, an important objective is to describe the motion of the ice cover in the Beaufort, Chukchi and Bering Seas.

B. Specific Objectives

The objectives of the research unit during **FY81** have been:

- (1) To modify the ice dynamics model developed by AIDJEX In order to improve the simulations of nearshore ice dynamics.
- (2) To produce specific oil spill trajectories using the modified model.
- (3) To incorporate the trajectories into oil spill scenarios.
- (4) To gather data in the **Chukchi** and Bering Seas **suitable** for testing future modeling efforts.

c. Relevance to Problems of Petroleum Development

Large portions of the Alaskan continental shelf are being considered for petroleum and gas development. An oil spill in these waters could have severe consequences for a number of wildlife species. A knowledge of the dispersion and transport of oil **spills** during the ice season can be used to develop cleanup plans and to protect sensitive wildlife areas. Ice motions also present a hazard to structures associated with offshore development.

III. CURRENT STATE OF KNOWLEDGE

The large-scale ice dynamics of the Beaufort Sea has been well characterized by the results of the **Arctice** Ice Dynamics Joint Experiment (**AIDJEX**) and subsequent modeling efforts (Pritchard, 1981). The range of **Beaufort** Sea ice motions has been identified by this research unit using historical atmospheric data and a free-drift ice model (Thomas and Pritchard, 1979). The pack ice can travel from near **Prudhoe** Bay to Point Barrow in a few months. Ice within the barrier island lagoons is fast for much of the ice season and moves only a limited distance, if at all. The motion of the ice in the transition zone between the fast ice and the Arctic pack (the shear zone) is not **fully** understood.

The behavior of oil spilled under or on sea ice is generally well understood from previous work by this research unit (Thomas, 1980). While details may not be well known, major surprises are not likely since the range of possible results appears to be limited.

Ice dynamics for the **Chukchi** and Bering **Seas** have not been studied as extensively as for the Beaufort Sea. We do know from buoy motions that considerable ice from the Bering Sea is advected northward through the Bering **Strait** into the **Chukchi** Sea (Thomas and Pritchard, 1981). Ice motions southward through the

Strait have also been observed several times each winter. The combination of winds, currents and ice strengths necessary for this southward ice breakout to occur is known (Reimer, et al., 1981), and it has been modeled successfully.

IV. STUDY AREA

Buoy deployments have been made in Norton Sound and in the **Chukchi Sea**. The modeling efforts are being focused on the nearshore Beaufort Sea.

V. SOURCES, METHODS AND RATIONALE OF DATA COLLECTION

The data collected by this research unit are being obtained by the use of ice drift buoys. The data are transmitted to the **TIROS-N** and **NOAA-A satellites**, then retransmitted by the satellites to ground stations and relayed to Service **Argos** in Toulouse, France. Service Argos decodes the messages, computes buoy locations and forwards the data to us by magnetic tape once a month. The data include buoy locations, ocean currents, and meteorological data. A description of the buoys deployed is given in Appendix A.

The buoys were deployed on the ice in Norton Sound by helicopter from **Nome**, in the **Chukchi Sea** by helicopter from Point Barrow, or by air drop from **fixed-wing** aircraft in the case of buoys which did not require that holes be drilled through the ice.

The winter 1980/81 Norton Sound deployment involved three deployments in January, February and March. This strategy was used to ensure adequate temporal coverage of the ice motion as the ice drifted out of the Sound.

The winter 1981/82 buoy deployment in Norton Sound also involved three deployments. These were made in December 1981 and in January and February 1982. These buoys provide us with a second winter's ice motion data which is necessary for determining interannual variability. In addition, the oceanographic and atmospheric sensors on some of the buoys deployed this year provide data adequate to estimate the effect of currents and winds on ice motion.

In the **Chukchi Sea**, two deployments were made, one in December 1981 and the second in February 1982. Two deployments were necessary because not all the buoys were available in December. The first deployment consisted of three air drop buoys, (TAD(A)) one of which contained a barometer. These buoys were air dropped due to concerns about the range of helicopters and the safety of landing **fixed-wing** aircraft on the ice in the **Chukchi** in early December. The barometer-equipped

buoy had developed an electrical problem during shipment and was not deployed at this time.

The second deployment consisted of three ADAP buoys with current meters, one of which also contained a barometer. The TAD(A) buoy from the first deployment, which had malfunctioned before deployment, was also put out at this time.

VI. RESULTS

A. Buoy Deployments

The 1981 Norton Sound buoy program was a complete success. The results of that program are contained in Flow Research Report No. 209 (Appendix B to this report.)

The 1982 Norton Sound buoy program has also been successful, with certain qualifications. A total of eleven buoys was deployed: two location-only buoys in December 1981, one location-only buoy and one met-ocean buoy in January 1982 and two met-ocean buoys and five location-only buoys in February 1982. The first met-ocean buoy deployed operated for only two weeks before transmission ceased. The last reported position of this buoy was off the mouth of the Yukon River, where heavy ice deformation commonly takes place. A search for this buoy was unsuccessful, but recent and heavy ridging was observed in the area and this is the most likely explanation for the total failure of the buoy. A second met-ocean buoy had an inoperative current meter, due to a faulty electrical connection. The buoy was relocated, but attempts to repair the buoy in the field did not succeed. Logistic concerns prevented a second attempt at repair. One position-only ADAP buoy also ceased transmitting, probably due to ice deformation. The remaining buoys have remained in operation until the present time. It is expected that all the buoys in Norton Sound will cease operating by June due to the melting of the ice cover.

During the December 1981 **Chukchi** Sea buoy deployment, it was discovered that one of the TAD(A) buoys was inoperative. This buoy was returned to the manufacturer for repairs and was successfully deployed during the second deployment in February 1982. Of the two TAD(A) buoys deployed in December 1981 one has worked according to specifications but the other has transmitted only infrequent and weak signals since the airdrop (according to personal communications with Service Argos).

In February 1982, four buoys were deployed in the Chukchi Sea. These included the TAD(A) with barometer that was not deployed during the first deployment and three ADAP buoys, all equipped with current meters for measuring currents 10 m beneath the ice. One of the **ADAPs** also contained a barometer. These four buoys were successfully deployed and operated as expected for about two weeks. At that time messages from two of the buoys indicated that the current meters had suddenly ceased operating. The data from the buoys indicated that there were open circuits between the ADAP units and the current meters. Both the speed and direction sensors were affected. Although it seemed most likely from the symptoms that these two current meters had been torn loose or disconnected by ice deformation, it was felt to be important to attempt to locate one of these buoys and determine the cause of failure in case it was due to design or manufacturing problems.

Four flights were made from Point Barrow for this purpose. A NOAA helicopter equipped with GNS navigation equipment was used for the search. Although we had frequent location fixes on the buoy from Service **Argos**, some of which were only three or four hours old and were accurate to a few hundred meters, the search was unsuccessful. The ice in the area where the buoy was thought to be had undergone extensive recent deformation. The 1-m-thick floe on which the buoy had been placed, which should have been apparent and readily located from the air, had been broken into many small pieces and heavily ridged (see Figure 1). Although we cannot be 100 percent certain, we still feel that ice deformation is the most likely reason for failure of the current meters.

A detailed description of the buoy deployments is given in Section IX of this report.

B. Modeling Work

No final results are available from the modeling work of this research unit. We have made a modification in the ice model to account for the effects of shallow water on the ocean drag felt by the ice. A preliminary report **of this** modification is appended to this report (Appendix C).

We have also obtained the 1979 and 1980 Arctic atmospheric pressure data from the World Data Center for **Glaciology**. A method has been devised for forming this data into coherent groups which represent different wind patterns over the Beaufort Sea. These wind patterns will be one of the parameters varied in our model.

A small-scale mesh has been laid out to cover the area in and about the **Diapir** lease area. The resolution of this mesh is about 10 km (see Figure 2.) To provide consistent boundary motions for this fine mesh, it will be nested in a larger mesh (Figure 3). The model using the coarse mesh will be driven by the same wind fields as for the fine mesh, and boundary motions for the larger area will be provided by interpolated **velocity** fields based upon drifting buoy data.

VII . DISCUSSION AND CONCLUSIONS

The specific objective of the modeling work being done by this research unit is to develop probable trajectories of oil spills occurring during the ice season in the nearshore region of the Beaufort Sea, i.e. , the **Diapir** lease area. **At first glance**, the magnitude of this problem seemed too formidable for **consideration**. One has not only to consider the range of winds at different times of the year, but ever-changing ice conditions must be accounted for. In fact, the ice conditions will depend upon the history of the winds. The only reasonable solution to the problem is a parameter study in which each of the factors which might significantly affect the oiled ice trajectories is varied over its range. The result is a **set** of short term, say daily, ice motions which can be combined into long-term trajectories with associated variability.

Previous work by this research unit (Thomas and Pritchard, 1979) has delineated the extremes of pack ice motion in the Beaufort Sea. Atmospheric data for 25 years were used to provide the means and variations of the driving forces for a free-drift ice model. The free-drift ice model itself accounted for one extreme of ice conditions: those conditions where internal ice stresses do not **play** a significant part. The other extreme , of course, is the situation where previous ice motion and ice growth has imparted a large compressive strength to the ice pack, and **little** or no motion occurs for certain wind conditions.

Throughout most of a typical year in the central Beaufort Sea, the free-drift ice motions mentioned above provide a reasonable approximation to large-scale spatial ice motions on monthly time scales. It is in the region near shore, where oil spills would be more likely due to drilling activity, that the ice will interact with the shore or immobile fast ice and cause very large variations in the long-term transport of the ice. For instance, some combinations of wind and **ice** conditions will result in ice deformation and grounded ridges, whereby oiled ice might be held in place through the winter, while other combinations would result

in oiled ice becoming incorporated into the pack and moving many hundreds of kilometers before summer. The total ice motion during the critical period might be only a few kilometers. Therefore, it is essential to look at the nearshore region on a much finer scale to resolve this critical period.

We will use a modified version of the ice model code developed during AIDJEX to compute the ice motions. One of the most important modifications to the model is a water drag law which takes into account the shallowness of the water over the shelf. A description of the water drag law is contained in Appendix C to this report.

Because of the cost of computations, we will use a quasi steady-state version of the model to determine daily ice motions. By this we mean that ice strength **will** not vary during the course of a calculation, and therefore ice strength must be one of the parameters which will be varied. Ice strength may be low, which is typical of early fall conditions when the ice is thin, it may be medium, as in the late fall or early winter, or strong, as in late winter.

Winds are a primary driving force of ice motions and must be included as one of the input parameters to be varied. The strength of the wind may be taken into account by introducing nondimensional variables. Then ice motions are seen to be dependent upon wind strength and fetch and inversely dependent on ice strength (Thomas and Pritchard, 1979). Thus, only the dimensionless group need be varied, which can be done by varying wind strength or ice strength. The fetch of the wind depends on the wind direction and the geometry of the region. The wind direction and overall pattern of the wind field are important parameters to be varied.

To derive typical wind fields for the Beaufort Sea, we have used the 1979 and 1980 daily atmospheric pressure fields reported by Thorndike and Colony (1980 and 1981). These pressure fields were derived using pressure data from an array of drifting buoys throughout the Arctic basin. The procedure we are using to derive typical wind fields is to first form distinct groups of daily pressure fields over the Beaufort Sea by visually examining the contour plots of atmospheric pressure and placing those with similar patterns into groups. Before proceeding further, the mean daily pressure for each day is subtracted from all the grid point pressure values so that what remains is a set of daily pressure field anomalies. A **multivariate** discriminate analysis technique **is** then used to refine the groupings and decide ambiguous cases. For each group, a mean pressure anomaly field is computed, from which we compute the geostrophic wind field and the surface winds.

These mean wind fields will then be used to drive the ice model. The wind patterns over the Beaufort Sea will be the parameter which is varied.

From the results of the ice model parameter study, we will be able to determine typical daily ice motions for different combinations of ice conditions and large-scale wind patterns. From the groupings of atmospheric pressure data, we will know for what percentage of the time each wind pattern can be expected during each part of the year as **ice** conditions change. From **this** information, we can then build up monthly or seasonal ice trajectories. Since the sequence of wind patterns over the Beaufort Sea will determine the ultimate ice trajectories in many cases, many different ice trajectories can be built up from one set of input parameters. This will enable us to obtain a range of possible ice trajectories due to variability in the temporal sequence **of** the winds. Additional variability will result from the variation in ice conditions input to the model.

VIII. NEED FOR FURTHER STUDY

One of the problems with the approach we are taking to the ice trajectory study is that we are assuming that ice conditions do not change during the course of a computation. We know that in the area near shore this approach can be misleading, but the cost of doing time-varying calculations is prohibitive. We will attempt to do at least one set of calculations where ice conditions do change during deformational events. This will allow us to compare our quasi steady-state calculations with a model which more closely simulates real sea ice. During the fall when the ice is thin and deformations can be large this time-dependent model may be especially important in delineating the development of the stamukhi zone.

The same kind of modeling effort and parameter study that we are doing for the Beaufort Sea must also be done for the **Chukchi Sea**. Since the **Chukchi** Sea is mostly covered by first-year **ice** during the winter, **ice** motion and deformation will likely be greater than in the Beaufort Sea except possibly for the nearshore region. The high speed ice motion **along** the northwest Alaskan coast is known to require a complete ice dynamics model for accurate simulation.

It is also important to continue the collection of data on ice motion and ocean currents **in** the **Chukchi** Sea in anticipation of modeling work and oil exploration activities. We have observed extreme variability in the ice motion in both the northern Bering and southern **Chukchi Seas**. Such **largevariabilityin**

such a small data set makes it difficult to estimate the typical behavior of ice or to be sure we have observed the complete range of behavior.

An effort was made this year to coordinate our deployment of ice-mounted current meters with the bottom-moored current meters put out by **RU91**. Not only should this coordination be continued, but early exchanges of data should be arranged to aid in data analysis and modeling. The buoys with barometers deployed in the **Chukchi** Sea also aid in refining the surface pressure analysis produced by the Polar Science Center based on an array of buoys in the Arctic.

In light of the importance of the wind on ice behavior, the more recent atmospheric pressure fields being produced for the Arctic should be acquired and analyzed. Data for the years 1979 and 1980 are being used in the present work, but the 1981 data is just now being processed (personal communication with Roger Colony). The historical data from **NCAR**, which is admittedly much less accurate but which spans about 30 years in the Arctic, should be compared with the more recent atmospheric data. This may provide information on the year-to-year variation in the winds as well as any medium-scale (tens of years) trends.

Ix. SUMMARY OF OPERATIONS

A. Chukchi Sea Buoy Deployment, 16-18 December 1981.

(1) Buoy Description

Three buoys were scheduled for deployment this trip. The buoys were TIROS Arctic Drifters, (TAD(A)), manufactured by Polar Research Laboratory, Incorporated, Santa Barbara, California. Two of the buoys (ID numbers 3620 and 3621) were position only buoys. The third buoy (ID number 3622) contained a barometer and compartment temperature sensor. All data from the buoys as well as buoy location is processed through Service **Argos**, Toulouse, France.

(2) Logistics

The buoys were deployed by air drop from the back of a Sky Van aircraft operated by Cape **Smythe** Air.

(3) Deployment Locations

Buoy #3620 was deployed about 33 nautical miles west of Barrow at **71.2°N, 158.5°W**. Buoy #3621 was deployed about 175 nautical miles west of Barrow at **71.6°N, 164.4°W**. Buoy #3622 was not deployed at this time.

(4) Ice Conditions

Ice conditions observed on the flight from Barrow to the drop positions consisted largely of new ice, with large amounts of open water and occasional older floes. Buoy #3620 was dropped **on** a floe about 6 to 8 kilometers in diameter. Buoy #3621 was dropped on a floe greater than 16 kilometers in diameter.

(5) Remarks

Buoy #3622 developed a loose connector inside the electronics package during shipment from Seattle and was returned to PRL for repairs. Buoy #3620 transmitted only weak and erratic messages after the air drop. Service **Argos** was able to obtain only a few unreliable position fixes for this buoy. Buoy #3621 has operated as designed.

(6) Scientific Personnel

Pete **Milovsoroff** of Flow Research Company made the buoy deployment.

B. Chukchi Sea Buoy Deployment, 7-16 February 1982

(1) Buoy Description

The buoys deployed during this trip were **Argos** Data Acquisition Platforms (ADA-P). All three buoys (ID numbers 3623, 3624, and 3625) were equipped with current speed and direction sensors. In addition, buoy #3625 also contained a barometer and compartment temperature sensor. The buoys are manufactured by Polar Research Laboratory, Incorporated, Santa Barbara, California.

One of the TAD(A) buoys, number 3622, which was not deployed during the December trip, was also put out at this time.

(2) Logistics

Buoy #3622, the air **droppable** TAD(A) was deployed using a Sky Van aircraft operated by Cape **Smythe** Air. The remaining three buoys were deployed using a helicopter (ERA Helicopter.)

(3) Deployment Locations

Buoy #3622 was air dropped approximately 240 nautical miles west of Barrow, at 71.1°N, 168.6°W. Buoy #3623 was deployed about 70 nautical miles west of Barrow at 71.2 °N, 159.0°W. Buoy #3624 was deployed about 30 nautical miles south of Point Hope at 67.9°N, 166.8°W. Buoy #3625 was deployed about 40 nautical miles northwest of Point Lay, at 70.1°N, 164.0°W.

(4) Ice Conditions

West of Barrow, on the way to deploy buoy #3622, the majority of the ice was relatively thin with some older floes. Ice compactness ranged from 50 to 75 percent. The buoy was dropped on a heavily ridged older floe.

Nearer the coast, where the other three buoys were deployed, there was a great deal of open water and heavily ridged first year ice. Buoy #3623 was deployed on a prominent floe about 1.5 kilometers in diameter and 94 cm in thickness. Buoy #3624 was deployed on a smaller floe, about 170 meters in diameter and 107 cm in thickness, in an area of much new and relatively thin ice. Buoy #3625 was deployed on a large floe several kilometers across and 61 cm thick.

(5) Remarks

Frequent bad weather caused delays in the deployment of these buoys but otherwise the operation was **sucessful**.

(6) Scientific Personnel

These buoys were deployed by Bob Pritchard and Pete **Milovsoroff** of Flow Research Company.

c. Chukchi Sea Buoy Retrieval Attempt, 14-17 March 1982.

(1) Purpose of Trip

After about two weeks of operation, buoys #3623 and 3624 began transmitting data indicating an open circuit in the current meter speed and direction sensors, i.e., zero count from the current meter rotor and magnetic north for the direction. The open circuit indication on the two buoys began within a few days of each other and approximately two weeks after deployment.

Two explanations were possible: ice deformation which may have destroyed the current meters, or failure of the buoy due to electrical or mechanical breaks in the cable between current meter and ADAP unit or a fault in the electronics of the ADAP itself. It was important to determine the exact cause of failure, since if it were due to failure of the buoy itself, the design or construction of future Arctic current meter buoys could be improved. It was therefore decided to attempt to locate buoy #3623, which was in a location convenient for helicopter search from Barrow. Since the buoy was still transmitting, accurate positions were usually available for the buoy from Service **Argos** within 3 to 6 hours of real time.

(2) Logistics

A NOAA helicopter equipped with Global Navigation System was used for the search. Four flights were made, two each on the 15th and 16th of March.

(3) Search Location

During the search, the buoy was at about **71°N, 167.7°W**, approximately 80 nm southwest of Barrow.

(4) Ice Conditions

In the area where the buoy was known to be, there was a great deal of recent ridging apparent. The 1-meter-thick floe on which the buoy had been deployed was found to be broken up into much smaller floes and into ice blocks in the ridge sails. A great deal of new ice approximately 30 cm or less in thickness was evident.

(5) Results

By obtaining a sequence of buoy fixes, it was possible to extrapolate the buoy motion and fly to within one kilometer (estimated) of the projected position using the helicopter's **Global** Navigation System. **This position was** marked so it could be located later, and a large area (about 50 square kilometers) about this point searched. This first projected buoy position could be compared with later buoy locations from Service Argos to obtain an estimate of the error which could then be used as a correction. On later flights the ice marked on the earlier flight could be located, then the

correction applied, assuming that the ice had recently moved as a rigid body with little rotation, and that the ice motion had been nearly linear. Observations seemed to confirm these assumptions. By repeatably applying this method, it was possible to locate the buoy position **to** within the accuracy of the buoy fixes from Service **Argos** (about 300 m) and the helicopter GNS (about **500 m**). This final area of less than one square kilometer was searched extensively but unsuccessfully. The only ice in the area which compared in thickness with the floe on which the buoy had been deployed, consisted of rubble and small floes. Figure 1 shows the search area, which three weeks earlier had been a 1-m-thick floe 1.5 km in diameter. Due to the large amount of recent ridging in the immediate area, we feel confident that ice deformation had sheared off or disconnected the current meter and hidden the **ADAP** unit amongst or adjacent to the ice blocks of a ridge sail.

(6) Scientific Personnel

The buoy search was made by Bob Pritchard and Pete **Milovsoroff** of Flow Research Company. The same personnel who made the buoy deployment also made the search in hopes they would be able to recognize the ice floe **on which** the buoy had been deployed.

D. Norton Sound Buoy Deployment, 16-19 December 1981.

(1) Buoy description

The buoys deployed on this trip were **Argos** Data Acquisition Platforms (**ADAP**). The buoy ID numbers were 3610 and 3611.

(2) Logistics

The buoys were deployed by helicopter (Bell 206). The operator was **Seair** Motive.

(3) Deployment Locations

Buoy #3611 was deployed 41 km southwest of Nome at **64.2°N** and **165.8°W**. Buoy #3610 was deployed 40 km south of Cape Darby at **64°N** and **162.6°W**.

(4) Ice Conditions

At this time a fast ice edge extended for about 2 km south of **Nome**. The ice immediately south of the fast ice edge was heavily **rubbled** with little open water. Further out in the sound the ice was relatively flat with thicknesses ranging from 20 to 50 cm. In the eastern part of Norton Sound the ice was thinner with extensive finger rafting and more open water.

(5) Remarks

On this trip the helicopter pilot felt that it was unsafe to venture more than about 50 km over ice with an average thickness of 20 to 50 cm and not at all over open water.

(6) Scientific Personnel

Jack **Kollé** of Flow Research Company made the deployments.

E. Norton Sound Buoy Deployment, 29 January - 5 February 1982.

(1) Buoy Description

Two **ADAP** buoys were deployed on this trip. Buoy #3612 was a position-only buoy. Buoy #3607 included measurements of current speed, current direction, floe rotation, **wind velocity and air temperature**. We refer to these as met-ocean buoys.

(2) Logistics

The buoys were deployed by helicopter (Bell 206). The operator was Seair Motive.

(3) Deployment Locations

Buoy #3612 was deployed 100 km south of Nome at **63.8°N** and **164.8°W**. Buoy #3607 was deployed 40 km northwest of Stuart Island at **63.8°N** and **162.4°W**.

(4) Ice Conditions

Ice conditions in Norton Sound were very similar to those reported for December. The fast ice edge was 2 to 3 km wide south of Nome and 50 km wide north of the Yukon Delta. The ice concentration in the western part of the sound was high with mostly **flat** ice 50 to 60 cm thick. Deformation of this

ice became more dominant near the fast ice edges. The ice in the area south of Cape **Darby** was quite thin, ranging from 10 to 20 cm thick. This ice was extensively finger-raftered as before. Considerable open water was observed in the southern and eastern parts of the sound on 5 February.

(5) Remarks

(6) Scientific Personnel

Jack **Kollé** and Don Thomas of Flow Research Company made these buoy deployments.

F. Norton Sound Buoy Deployment, 23 February - 5 March 1982.

(1) Buoy Description

Seven **ADAP** buoys were deployed on this trip. **Two were met-ocean buoys** (ID numbers 3608 and 3609) and the remainder were position-only (ID numbers 3613 through 3617).

(2) Logistics

The buoys were deployed by helicopter (Bell 206). The operator was **Seair** Motive.

(3) Deployment Locations

Buoy #3608 was deployed 60 km south of Nome at **64.0°N** and **165.0°W**. Buoy #3613 was deployed on the fast ice north of the eastern end of St. Lawrence Island at **63.5°N, 165.0°W**. Buoy #3609 was deployed 40 km southwest of Cape **Darby** at **64.0°N, 163.5°W**. Buoy #3614 was deployed on the fast ice of the Yukon Delta 45 km north of the coast at **63.5°N, 164.5°W**. Buoy #3615 was deployed on a fast ice remnant which had drifted to a spot 25 km southeast of Nome at **64.2°N, 165.1°W**. Buoy #3616 was deployed 30 km southwest of Cape Darby at **64.0°N, 163.2°W**. Buoy #3617 was deployed on a large rubble pile on the east side of Sledge Island at **64.5°N, 166.1°W**.

(4) Ice Conditions

During this time ice conditions were considerably different from those observed on the two previous trips. The fast ice south of Nome had drifted

south into the Sound to be replaced by multiply rafted thin ice. The ice south of Nome was more deformed and the deformation extended further out into the center of the sound. The fast ice of the Yukon Delta had not changed appreciably. The ice in the eastern part of the sound was also more deformed and less uniform. The bulk of the ice here was still flat and rafted. Open water was not observed in **large** amounts except in the extreme eastern portion of the sound. Large ice hummocks were observed in the Yukon fast ice and near Sledge Island. On a flight to St. Lawrence Island extensive flat and rafted ice was observed.

(5) Remarks

An attempt was made to locate buoy #3607 which had ceased transmitting on February 20. The ice in the search area was heavily deformed and it was not possible to locate the buoy.

After deployment, the current meter **on** buoy #3609 failed to operate. An **unsuccessful** attempt was made to locate this buoy on 2 March using RDF headings. On 3 March the buoy was found using compass headings off Cape **Darby** and Rocky Point. The electrical cable to the current meter was found **to** be disconnected. The connection was remade and the current meter was redeployed using a separate rope **to** avoid any strain on the **connection**. Unfortunately, approaching darkness and **visual** flight rules prevented any further work or testing of the buoy. Later, data from Service Argos showed that there was again an open circuit between the **ADAP** unit and the current meter.

Future deployments of these complex buoys should allow for relocating buoys for repair and inspection. Buoys should be well marked and the aircraft should be equipped with accurate navigation equipment.

None of the pilots involved in these deployments had any experience in the Norton Sound area. A knowledge of local conditions is critical to safe and efficient operations under these difficult conditions. The use of inexperienced pilots and lack of adequate navigation gear resulted in severely limited helicopter range, ground delays, and rushed deployments. The latter was the most important factor in the current meter failure on buoy #3609.

(6) Scientific Personnel

Jack **Kollé** of Flow Research Company made the buoy deployments. **Lew** Shapiro and Sam Yang of ARCO aided **in** deployment of the met-ocean buoys and ice reconnaissance.

REFERENCES

- Pritchard, R. S. (1981) "**Mechanical** Structure of Pack Ice," in Mechanics of Structured Media, Proceedings of the International Symposium on the Mechanical **Behaviour** of Structured Media, Ottawa, May 18-21, pp. 371-405.
- Reimer, R. W., Schedvin, J. C., and Pritchard, R. S. (1981) "**Chukchi** Sea Ice Motion", in POAC 81, The Sixth International Conference on Port and Ocean **Engineering under Arctic Conditions**, Quebec, Canada, Vol. II, pp. 1038-1046.
- Thomas, D. R. (1980) "Behavior of Oil Spills under Sea Ice-Prudhoe Bay," Flow Research Report No. 175, Flow Research Company, Kent, Washington.
- Thomas, D. R., and Pritchard, R. S. (1979) "**Beaufort** and **Chukchi** Sea Ice Motion, Part 1. Pack Ice Trajectories," Flow Research Report No. 133, Flow Research Company, Kent, Washington.
- Thomas, D. R., and Pritchard, R. S. (1981) "Norton Sound and Bering Sea Ice Motion-1981," Flow Research Report No. 209, Flow Research Company, Kent, Washington.
- Thorndike, A. S., and Colony, R. (1980) "Arctic Ocean Buoy Program Data Report 19 January 1979 to **31** December 1979," Published by the Polar Science Center, University of Washington, Seattle, Washington.
- Thorndike, A. S., and Colony, R. (1981) "Arctic Ocean Buoy Program Data Report 1 January 1980 to 31 December 1980," Published by the Polar Science Center, University of Washington, Seattle, Washington.

SUPPLEMENTARY MATERIAL

A. Meetings Attended

- (1) Robert Pritchard and Don Thomas attended the OCSEAP synthesis meeting at **Chena** Hot Springs, Alaska, 20-23 April, 1981.
- (2) Robert Pritchard and **Jack Kollé** attended POAC 81 (The Sixth International Conference on Port and Ocean Engineering under Arctic Conditions) in Quebec, Canada, 27-31 July, 1981.
- (3) Robert Pritchard and Don Thomas attended an OCSEAP review meeting at Lake Wilderness, Washington, 27-28 January, 1982.

B. Publications

- (1) Pritchard, R. S. (1981) "Mechanical Structure of Pack Ice." in Mechanics of Structured Media, Proceedings of the International Symposium on the Mechanical **Behaviour** of Structured Media, Ottawa, May 18-21, pp. 371-405.
- (2) **Reimer**, R. W., **Schedvin**, J. C. , and Pritchard, R. S. , (1981) "**Chukchi** Sea Ice Motion," in POAC 81, The Sixth International Conference on Port and Ocean Engineering under Arctic Conditions, **Quebec**, Canada, Vol. II, pp. 1038-1046.



Figure 1. View of the Area Where Bouy Number 3623 was Determined to be. Ridge in Foreground was Estimated to be 5m High and is Composed of Ice **Blocks** About **1m** Thick.

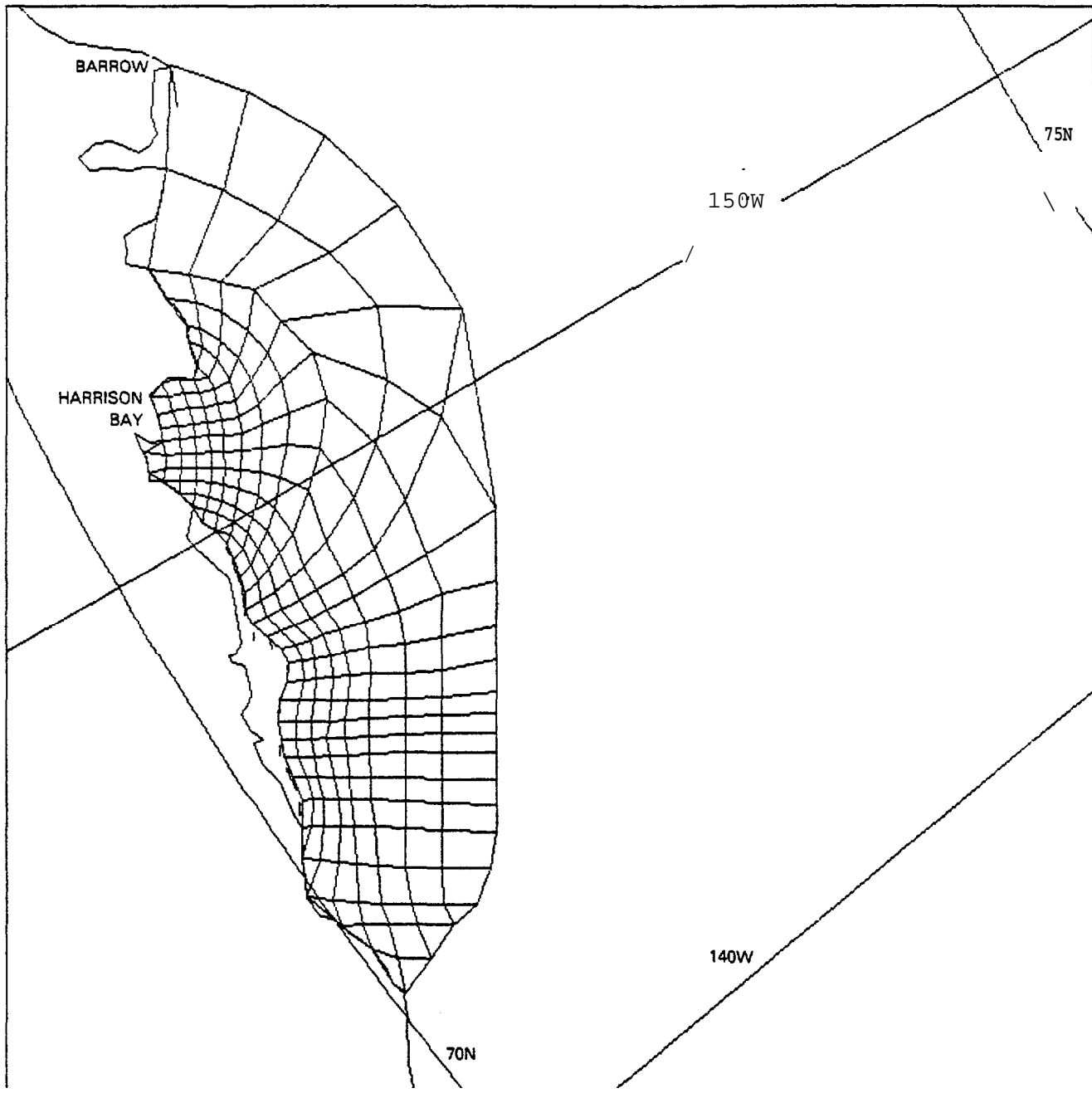


Figure 2. Small Scale **Computational** Grid for the Ice Motion Simulation Study. Grid Covers an Area About 150 km by 550 km in Size, Elements are from 7 km to 30 km in Size.

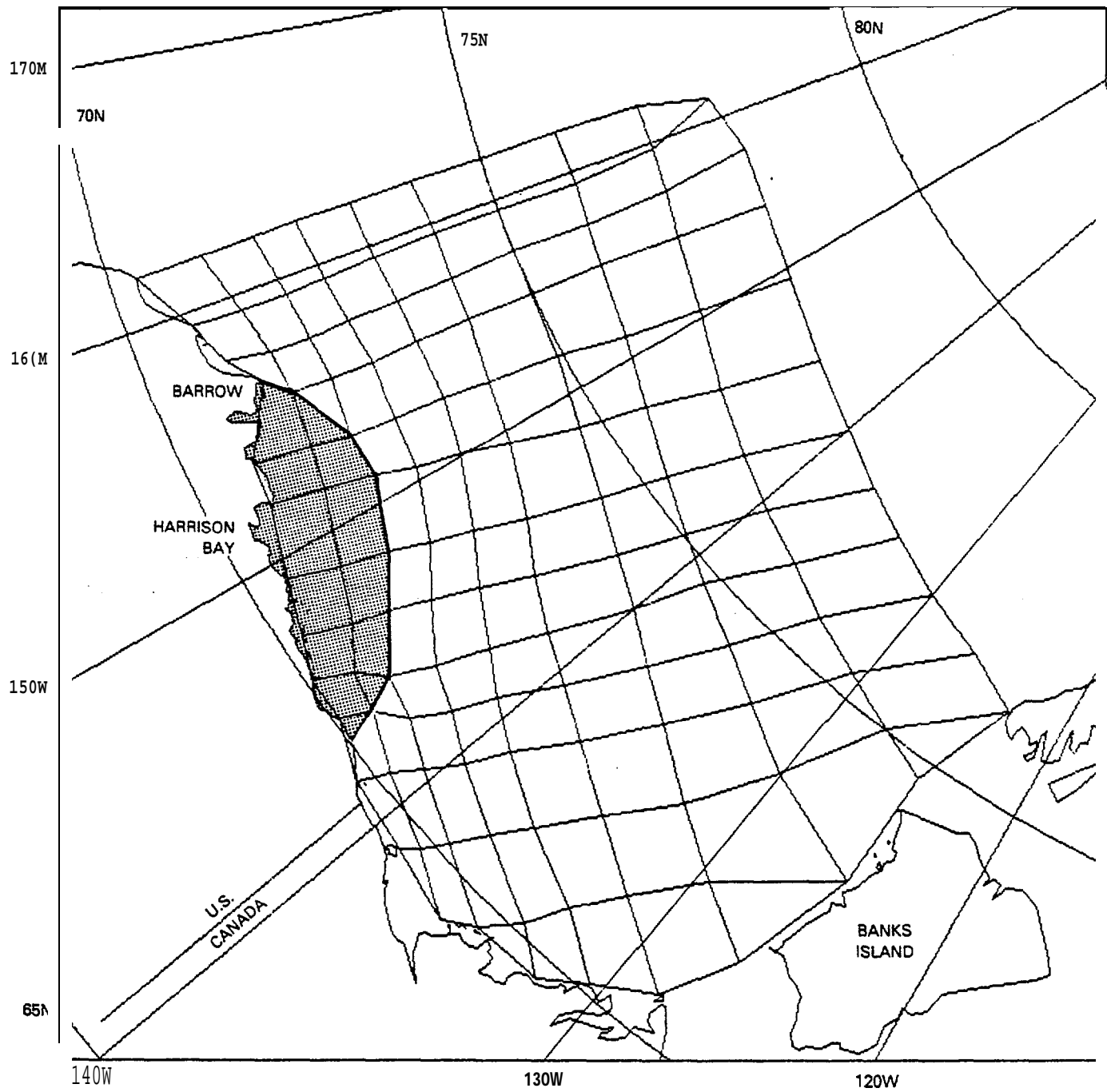


Figure 3. Large Scale Computational Grid Used to Provide Boundary Motions for the Small Scale Grid. Grid Covers an Area of 1000 km by 1400 km with Elements from 50 km to **100** km in Size.

APPENDIX A
BUOY DESCRIPTIONS

The buoys used by this research unit are manufactured by Polar Research Laboratory, Incorporated (PRL), Santa Barbara, California, and are based on the PRL **Argos** Platform Transmit Terminal (**PTT**) model 801 electronics package. This PTT is designed to operate with the Argos system aboard the **TIROS/N** and **NOAA/A** series of satellites. The **Argos** system provides a telemetry link between data acquisition platforms and the user. In addition, the Argos system can provide the position of the platform which is based on the **doppler** shift of the transmitted message and the known position of the satellite at the time of **transmission**. Accurate determination of position depends upon a stable oscillator of known frequency. The PTT 801 operates at a frequency of 401.65 MHz (**+ 1.25 kHz**) with a long-term stability of less than 1.20 **kHz/year**. The temperature range of this PTT is from **-50°C to +40°C**. Lithium battery packs were used in order to provide operational lives of six months or more.

In operation, the PTT transmits a signal every 60 seconds. The signal is from 360 to 920 ms in duration, depending on the number of sensors. The platform ID and up to 256 bits of data are transmitted each 60 seconds. The data format consists of from one to eight data frames where each frame typically consists of four 8-bit words.

The PTTs used were in two configurations, the Argos Data Acquisition Platform (**ADAP**) and the TIROS Arctic Drifter in a parachute deployable form (**TAD(A)**). The ADAP is a portable, self-contained unit intended for hand deployment. The ADAP is packaged in a waterproof polyethylene case measuring 41 cm on a side and weighing 19.2 kg. The ADAP itself contains no sensors but will handle up to 32 sensors.

The TAD(A) is housed in a hollow, insulated fiberglass sphere about 60 cm in diameter and weighs about 36.4 kg. An inner structure that carries the electronics, antenna and batteries rides on **teflon** buttons that serve as a gimbal system. Counterweights cause the inner structure to rotate within the outer sphere so that the antenna ground plane is **in** a horizontal position regardless **of** the attitude of the outer shell. A crushable foam cushion serves to limit deceleration loads. A switch within the cushion is closed upon impact which fires an explosive cable cutter to release the parachute.

Counterweights cause the inner structure to rotate within the outer sphere so that the antenna ground plane is in a horizontal position regardless of the attitude of the outer shell. A crushable foam cushion serves to limit deceleration loads. A switch within the cushion is closed upon impact which fires an explosive cable cutter to release the parachute.

A variety of sensor packages were used with the buoys deployed during 1981-82. Many of the buoys were position only buoys in either the hand deployable ADAP or airdropable TAD(A) configurations. These buoys are relatively cheap and provide a means of tracking ice motions. The positional accuracy of these buoys has a radial standard deviation of about 300 m.

Two of the buoys deployed in the **Chukchi** Sea contained barometers. The barometers are manufactured by **Paroscientific**, Redmond, Washington. The barometers utilize a quartz beam whose frequency of vibration is dependent on atmospheric pressure. The temperature inside the barometer housing is also sensed by a thermistor. This reading is processed through Argos and is used to correct the barometer reading for temperature effects.

Three of the buoys deployed in the **Chukchi** Sea during 1982 and three of those deployed in Norton Sound in 1982 contained sensors for current speed and direction. The current meters are a product of **Marinco, Incorporated**, a subsidiary of Intersea Research Corporation, San Diego, California. Current speed is sensed by a Savonius Rotor. Current speed is measured by counting the cycles from the **Savonius** Rotor. The maximum speed to be measured was chosen to be 3 knots. When the speed is encoded into an 8-bit word, the increment in current speed is $3/256$ knots, or approximately 0.011 knots.

Current direction is sensed by a plastic vane assembly attached to the body of a potentiometer, the shaft of which is rotated by a magnetic compass. The resistance of the potentiometer varies then according to the current direction with respect to magnetic north. The current direction is also encoded into an 8-bit word, so the incremental step in current direction is $360/256$ degrees.

Three of the 1982 Norton Sound buoys included sensors for wind speed, wind direction and air temperature. Since wind direction was measured relative to the rigid mast assembly mounted on the ice, a compass was also included to give floe orientation. The cup anemometer and wind vane are products of Weather Measure Division, Sacramento, California. The anemometers are DC generator types, generating 1 volt DC at 100 MPH. Wind direction is sensed by a vane attached to a

To obtain more accurate representations of the steady winds and currents, all sensor data except for the barometers and internal temperature sensors were averaged by hardware within the buoy before being transmitted. In order to reduce power consumption, it was also decided to obtain new samples from the sensors and thus a new average once every two hours. The length of time over which a current speed sample is taken is 8.21 seconds. The sample taken by the other sensors are instantaneous. The sensors are sampled 32 times, once every 16 seconds over a period of about 9 minutes.

In order to insure a more continuous series of data, a total of four averages for each sensor is retained in an internal memory of the buoy and are transmitted in turn every 60 seconds. That is, the buoy will first transmit the newest data (that sensed and averaged within the last two hours), then 60 seconds later it will transmit the data taken two hours before the most recent, then 60 seconds later the data taken 6 hours before the most recent then 60 seconds later the data taken 4 hours before the most recent. This cycle is repeated every four minutes until a new sample of data is taken and averaged. **A transmission counter is included as a sensor in order to determine which two hour data sample is being transmitted. The very first data sample is taken during the nine minutes after the buoy is first turned on. By this means we are assured of obtaining a more continuous series of data points every two hours, even during those times when a buoy may not be seen by a satellite.**

-B1-

APPENDIX B

Flow Research Report No. 209, "Norton Sound and Bering Sea Ice Motion-1981"
is included as Appendix B.

REGISTERED

RU-568

Flow Research Report No. 209
Norton Sound and Bering Sea
Ice Motion: 1981

by

D. R. Thomas
and
R. S. Pritchard

October 1981

Flow Research Company
A Division of Flow Industries, Inc.
21414-68th Avenue South
Kent, Washington 98031
(206) 872-8500

Acknowledgement

The authors thank Ms. K. L. Hammond for her extensive writing and editing efforts on this **report**. This study was supported by the Bureau of Land Management through interagency agreement with the National Oceanic and Atmospheric Administration, under which a **multiyear** program responding to the needs of petroleum development of the Alaskan Continental Shelf is managed by the Outer Continental Shelf Environmental Assessment Program (OCSEAP).

Table of Contents

	Page
Acknowledgement	i
List of Figures	111
1. Introduction	1
2. Data Acquisition and Processing	4
3* Buoy Deployments	6
3.1 January Deployment	6
3.2 February Deployment	8
3.3 March Deployment	8
4. Results	9
4.1 Buoy Trajectories	9
4.2 Discussion	18
5. Conclusions	19
6. References	20
Appendix: Buoy Position Data	21

List of Figures

	Page
Figure 1. Norton Sound Buoy Deployment Pattern. Buoys 3600, 3601, and 3602 Were Deployed January 18-20, 1981 (Days 18-20); Buoys 3603 and 3605 Were Deployed February 20-21, 1981 (Days 51-52); Buoys 3604 and 3606 Were Deployed March 16, 1981 (Day 75).	7
Figure 2. Trajectory of Buoy 3600 from January 18 to May 23, 1981 (Days 18 to 143)	10
Figure 3. Trajectory of Buoy 3602 from January 18 to May 10, 1981 (Days 18 to 130)	11
Figure 4. Trajectory of Buoy 3601 from January 20 to April 29, 1981 (Days 20 to 119).	12
Figure 5. Trajectory of Buoy 3603 from February 21 to June 19, 1981 (Days 52 to 169).	13
Figure 6. Trajectory of Buoy 3605 from February 20 to April 1, 1981 (Days 51 to 91)	15
Figure 7. Trajectory of Buoy 3604 from March 16 to May 23, 1981 (Days 75 to 143).	16
Figure 8. Trajectory of Buoy 3606 from March 16 to May 15, 1981 (Days 75 to 135).	17

1. Introduction

As oil exploration activity increases in Norton Sound and the eastern Bering Sea, it becomes important to know the expected and extreme sea ice conditions in this region. These conditions will determine the drilling and shipping seasons and the design of offshore structures and vessels which may operate in the area. A limited understanding of the general conditions in this area has been derived using satellite images as the data source. However, the information obtained from satellite imagery is not sufficient to enable predictions of probable or possible extreme events which could be hazardous to shipping or drilling operations. A complete data set of the ice conditions in the Norton Sound area is required to better understand and predict future events.

Generally, the sea ice found in Norton Sound is relatively thin ice (less than 1 m thick) that may be moving at high speeds, up to 50 km per day. The ice is formed inside the sound along the northern edge and in Norton Bay. This ice is advected south and west through the sound, growing thicker due to thermal growth and by rafting of thin ice. As the ice leaves the sound it makes a sharp bend, either to the north following the northward flowing currents or to the south under the influence of the predominantly northerly winds. Pease (1980) has suggested that Norton Sound may produce an area of ice during one ice season that is from 2 to 10 times the area of the sound, depending upon atmospheric events.

Large ice rubble features form in Norton Sound where the moving ice cover impinges upon the shore or grounded shorefast ice. Kovacs (1981) observed several of these features in the spring of 1980. Many were grounded in water about 10 m deep and extended up to 14 m above the surface. Laterally, these rubble piles had dimensions up to a few hundred meters. The largest concentrations were found off the mouth of the Yukon River, but they were also found near Sledge Island, Stuart Island, off the north side of St. Lawrence Island where strong westerly winds could drive them into Norton Sound and even in Norton Bay. Kovacs also gives accounts of several of these rubble piles which were afloat and moving (apparently with the currents). These drifting rubble piles represent the extreme ice hazard which a ship or drilling structure might encounter.

In addition, thicker Arctic pack ice (2 to 3 m thick) from the Chukchi Sea may be carried southward through the Bering Strait during periods of current reversals. Generally, the currents through the Bering Strait flow to the north. Several times each winter, however, the currents in the Bering Strait will reverse for several days, flowing to the south (Coachman and Aagaard, 1981). Reimer, Schedvin and Pritchard (1981) have modeled ice conditions in the Chukchi Sea during one of these current reversals and have shown how ice in the Chukchi Sea could pass through the strait as a result of a current reversal. Thus, based upon our present state of knowledge, it is possible that multiyear ice or heavily ridged first-year ice could move south through the Bering Strait and into the outer portion of Norton Sound. This Arctic pack ice, which may include some large ridges, could possibly enter Norton Sound during westerly wind and eastward current conditions. The probability of this occurring is low, but more ocean current data for Norton Sound and the eastern Bering Sea are needed for verification. A better understanding of the ice drift caused by currents and winds is also needed.

Most of the recent work on Norton Sound ice conditions has utilized satellite images as the data source (Stringer, 1980; McNutt 1981). While these studies account for most of our knowledge of the ice conditions in this area, there are limitations to the information contained in satellite imagery. NOAA satellite images provide daily coverage of the Norton Sound area, but the spatial resolution (on the order of 1 km) allows identification of only very large ice features. LANDSAT imagery provides much better spatial resolution (about 80 m), but due to orbit precession, the Norton Sound area is imaged for only 2 or 3 days during each 18-day period. Cloud cover is another factor which often limits the usefulness of these satellite images.

Satellite images have been used primarily to give areal coverage of ice of different types or thicknesses. For example, the extent of landfast ice, the area of open water, thin ice or thick ice and the nature of the ice cover, whether loose floes, solid ice sheet, etc., can all be observed on satellite images. Some information on ice motion has also been taken from satellite imagery (McNutt, 1981), but the results are limited in spatial coverage and are not continuous in time.

A complete set of ice motion data for the Norton Sound area during the winter of 1980-81 now exists. This report describes the buoy deployment

program used to obtain this data and presents the results of the program. The complete data set has also been submitted to the National Oceanographic Data Center (NOOC), and interested investigators may obtain the data from that source.

*National Oceanographic Data Center, Page Building No. 1, 2001 Wisconsin N.W., Washington, D.C. 20235

2. Data Acquisition and Processing

The buoys deployed in this study were standard **Argos** Data Acquisition Platforms (**ADAP**) manufactured by Polar Research Laboratory, Inc., of **Santa** Barbara, California. To report its position, each buoy transmitted an identification number at 1-rein intervals at a fixed frequency. When a satellite (**TIROS-N** or **NOAA-A**) was in **radio** sight of the buoy, this message was received by the satellite, but with a frequency shift due to the Doppler effect. This Doppler shift is caused by the relative motion of the buoy and the satellite. The size of the frequency shift, **together** with the known satellite orbit, suffices to determine the location of the buoy. Buoy positions were processed by Service **Argos** in Toulouse, France.

Each buoy was packaged in a polyethylene case in a **configuration** that is unstable if it hits open water. This instability causes the buoy to turn upside down, with its antenna underwater. Although the buoy **will** continue to float for a short time, it will not be able to report its position. For this study, the first buoy was deployed January 18, 1981, and the last buoy ceased operation on June 19, 1981.

From the beginning of the experiment through February 27, both the **TIROS-N** and **NOAA-A** satellites were functioning. During this time, an average of about 11 fixes per day was obtained. After February 27, when **TIROS-N** was shutdown, approximately six fixes per day were obtained. Generally, the longest period between fixes was 12 hours or less. On March 19, a data transmission line failure resulted in the loss of some data, with a period of 42 hours between fixes.

The quality control and editing of data by Service **Argos** has proven to be adequate. In addition, visual checking for errors was performed to look for impossible positions or displacements; none were found. Service **Argos** states a standard deviation in position error of the satellite positioning system to be 700 m. During preliminary checkout of the buoys at the Nome Airport, 20 positions of the seven buoys were obtained. Two-thirds of the fixes were within a radius of 300 m, and all were within a maximum error of 800 m. These numbers compare favorably with the error analysis of **Thorndike** and Colony (1980).

To facilitate presentation of the data and to remove short-time-scale tidal and inertial oscillations, the data were filtered with a 24-hour cosine

-5-

filter. Daily positions, $X(0)$, were computed at 0000 hours Greenwich Mean Time (GMT), $T(0)$. The time differences, $AT(i)$, were computed as

$$AT(i) = T(i) - T(0) \quad (1)$$

for all $T(i)$ within 24 hours of $T(0)$. The daily positions were then computed as

$$x(0) = \frac{\sum X(i) W(i)}{\sum W(i)}, \quad (2)$$

where the weights, $W(i)$, are defined as

$$W(i) = \cos \left[\Delta T(i) \frac{\pi}{24} \right]. \quad (3)$$

Daily displacements or, equivalently, average daily velocities were then obtained by differencing the daily positions and converting from degrees to kilometers.

3. Buoy Deployments

Seven automatic data buoys were deployed in the Norton Sound area to obtain ice motion data for a complete winter season. Three deployments were made at approximately one-month intervals during the period from January through March 1981. All buoys were deployed by helicopter from Nome, Alaska. They were deployed either within Norton Sound or just outside the mouth of the sound.

The buoy deployment pattern is shown in Figure 1. Three buoys, identified as 3600, 3601 and 3602 in the figure, were deployed during January 18-20, 1981. As these buoys drifted out of Norton Sound into the northern Bering Sea, two more buoys, identified as 3603 and 3605, were deployed as replacements. This second deployment took place on February 20-21, 1981. Finally, as these two buoys drifted westward out of Norton Sound, two more buoys were deployed to replace them. The buoys identified as 3604 and 3606 were deployed on March 16, 1981. Each deployment is described more completely in the following subsections.

3.1 January Deployment

On January 18, 1981, buoy 3602 was deployed just inside the mouth of Norton Sound and buoy 3600 was deployed about 80 km to the west, just outside the mouth of the sound. The air temperature was about -12°C and very little open water was observed, except for one large lead several kilometers wide extending as far as could be seen to the north and south. This lead was right in the mouth of Norton Sound, between buoys 3600 and 3602. In general, ice conditions consisted of thick snow-covered floes (estimated to be at least 0.5 m thick) in a matrix of much thinner new ice. The thin ice was heavily rafted and ridged.

On January 20, 1981, buoy 3601 was deployed in the eastern part of Norton Sound (southeast of Cape Darby). This buoy was the easternmost one deployed during this study. All the ice in this part of the sound consisted of very young, thin ice (10 to 30 cm thick) except where rafting had occurred. A great deal of rafted ice and open water was present, indicating a recent history of ice motion.

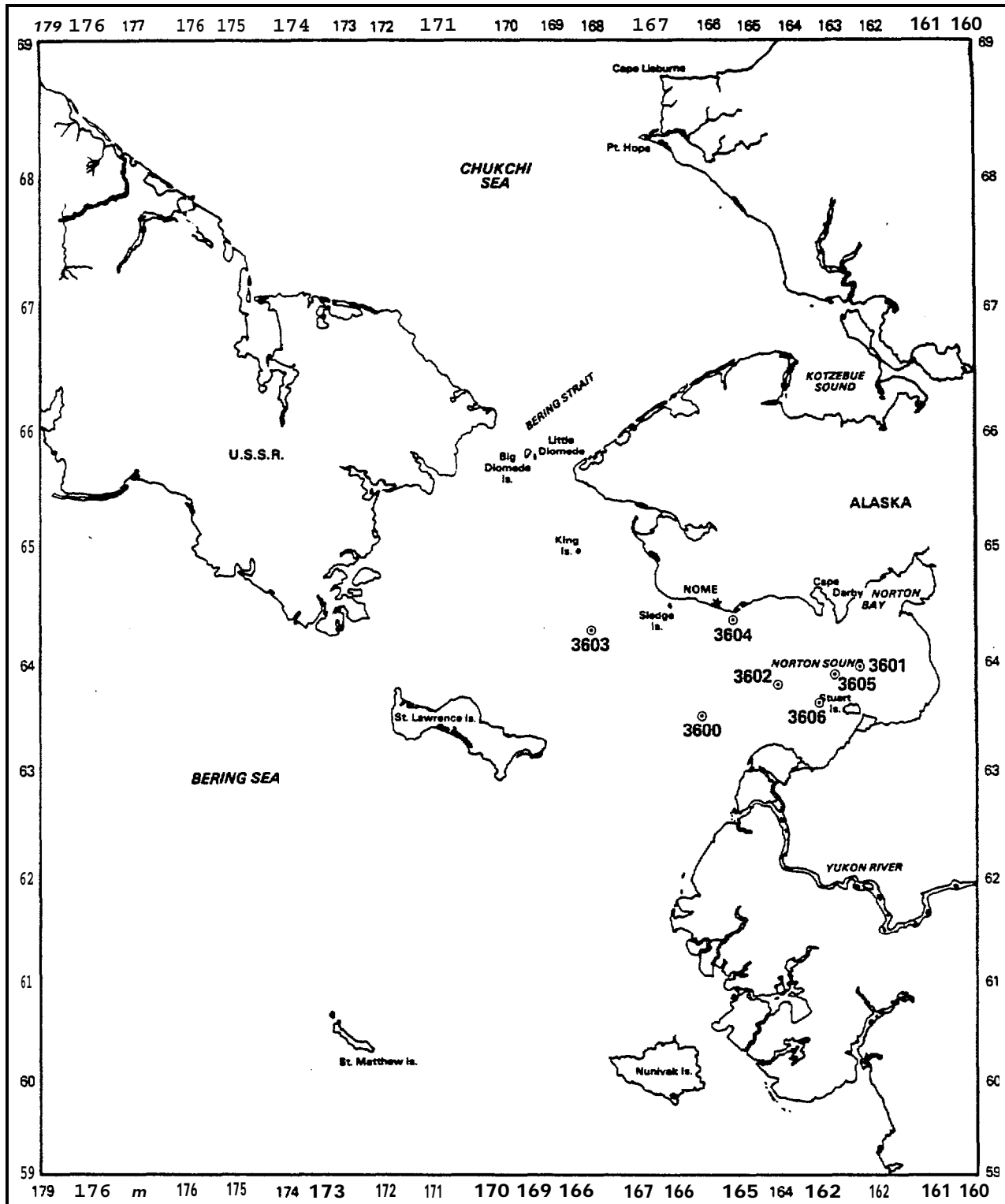


Figure 1. Norton Sound Buoy Deployment Pattern. Buoys 3600,3601, and 3602 Were Deployed January 18-20,1981 (Days 18-20); Buoys 3603 and 3605 Were Deployed February 20-21,1981 (Days 51-52); Buoys 3604 and 3606 Were Deployed March 16,1981 (Day 75).

3.2 February Deployment

Buoy 3605 was deployed on February 20, 1981, approximately 50 km south of Cape Darby. From Nome to Cape Darby open water was observed to about 1 km from the shore. The air temperature was approximately -13°C and the water was freezing constantly. A north wind kept the lead open by finger rafting the thin ice and pushing it south. The ice became continuously thicker south of the shoreline. A flat ice thickness of 26 cm was measured 50 km south of Cape Darby. This ice was rafted in places to a thickness of 50 cm or more.

On February 21, 1981, buoy 3603 was deployed about 150 km due west of Nome. Inside Norton Sound, ice pileups 10 m high or more were observed on a shoal and on the shore of Sledge Island. Flat ice thickness was estimated to be 20 to 30 cm. A 1- to 2-km-wide lead extended north-south as far as could be seen west of Sledge Island. Thick, snow-covered, old ice was observed at the deployment site due south of King Island. This ice was at least 1 m thick and ridged along floe boundaries to 5 or 6 m in thickness.

3.3 March Deployment

Buoys 3604 and 3606 were deployed on March 16, 1981. Daytime temperatures were just above freezing (0 to 1°C), but the temperature dropped to below freezing at night. All the ice observed beyond the shorefast ice was thin (estimated to be 10 to 20 cm) and contained much open water. This condition seemed to exist throughout the sound with the amount of open water decreasing to the south. A large shore lead existed between the fast ice and the pack along the north coast of the sound.

4. Results

4.1 Buoy Trajectories

The trajectories of each data buoy deployed on the ice cover in Norton Sound are presented in Figures 2 through 8. These ice motion histories were calculated using the smoothed daily positions and average daily velocities which were obtained as described in Section 2 (a complete list of these data is provided in the Appendix). In the figures, daily buoy positions at 0000 hours GMT are indicated with black dots on the trajectories, and Julian days at 20-day intervals (with January 1, 1981 = day 1) are also indicated.

In Figure 2 we present the motion of buoy 3600 from Julian days 18 through 143. The buoy was deployed in the mouth of Norton Sound about 130 km south of Nome. During the first 20 days, this buoy alternately moved north then south but with a gross motion toward the west. After that period, large south-westward motions occurred for about 40 days. Finally, for roughly 60 days a northwestward motion in the southern Bering Sea took place until the buoy ceased reporting on Julian day 143, presumably when it reached the ice edge.

In Figure 3 we present the motion of buoy 3602 beginning on Julian day 18 and ending on day 130. This buoy was deployed just inside the mouth of Norton Sound about 80 km east of buoy 3600. Buoy 3602 drifted westward during the first 20-day period, then for 40 days it moved to the southwest, as did buoy 3600. After that time, buoy 3602 made a large clockwise, circular motion remaining south of St. Lawrence Island but moving back to the northeast. It ceased to function on day 130.

In Figure 4 we present the motion of buoy 3601, which was deployed in the eastern portion of Norton Sound north of Stuart Island. This buoy also drifted westward out of Norton Sound during the first 20-day period. It drifted to the southwest along with buoys 3600 and 3602 between days 40 and 80 and then reversed its course generally towards the northeast for 20 days, although the gross motion during this time was small.

In Figure 5 we present the motion of buoy 3603, which was deployed outside of Norton Sound to the west of Nome on Julian day 52. Soon after day 60, this buoy began traveling northward toward the Bering Strait. After approximately 1 week, it then reversed its course and by day 80 it had moved south of

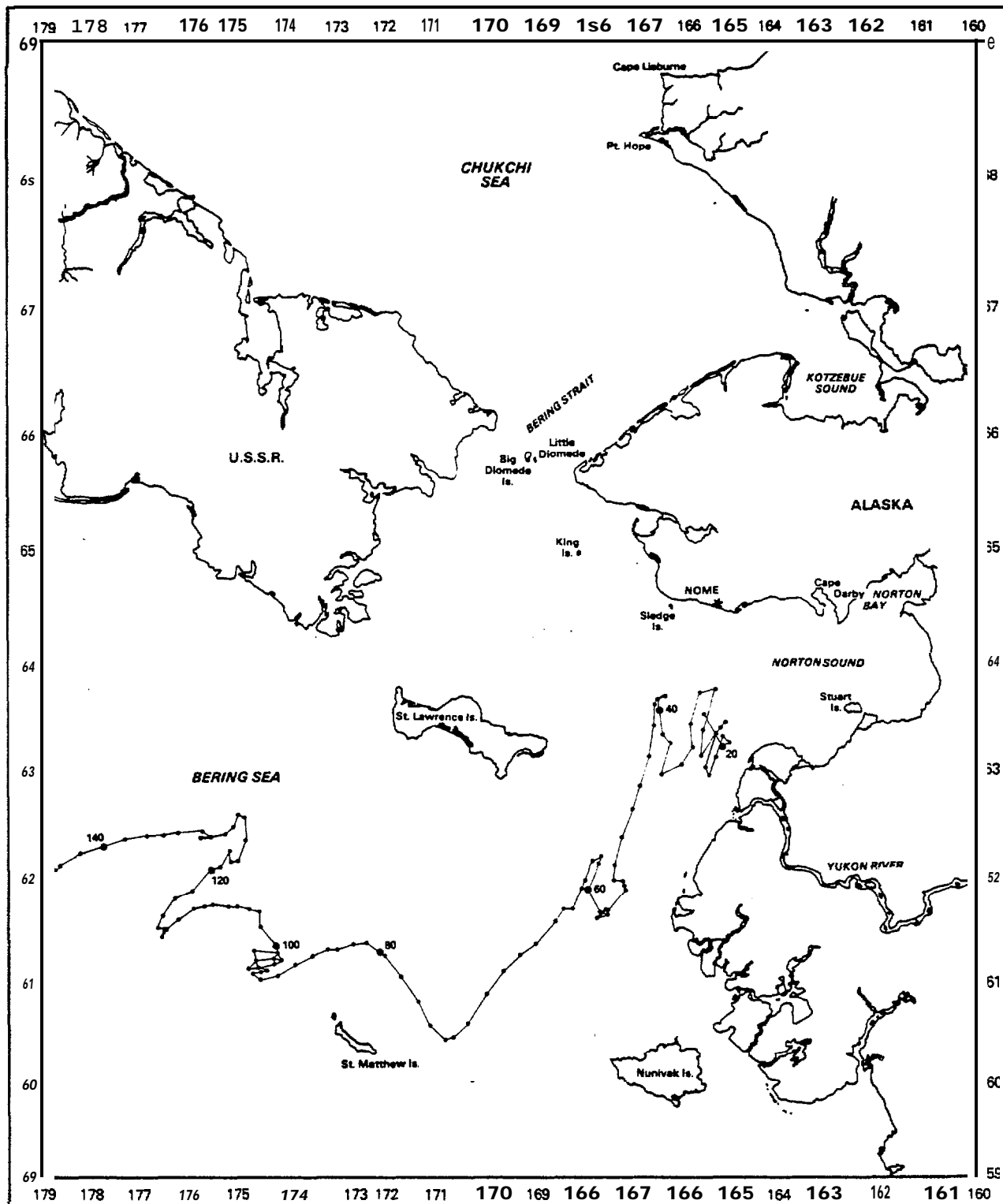


Figure 2. Trajectory of Buoy 3600 From January 18 to May 23, 1981 (Days 18 to 143). Daily Positions at 0000 Hours GMT Are Marked with Dots and Julian Days at 20-day Intervals Are Identified.

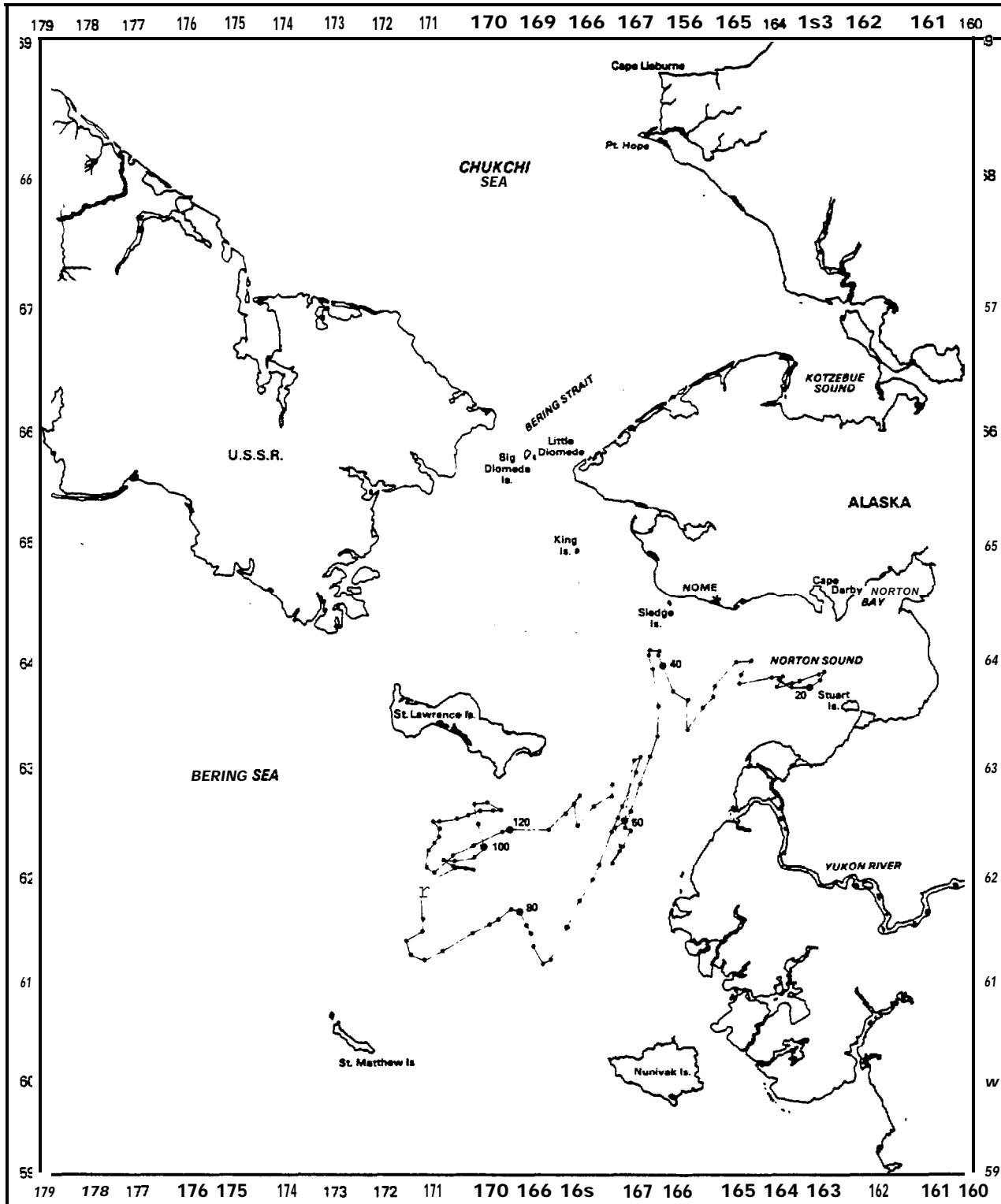


Figure 3 . Trajectory of Buoy 3602 from January 18 to May 10, 1981 (Days 18 to 130). Daily Positions at 0000 Hours GMT Are Marked with Dots and Julian Days at 20-day Intervals Are Identified.

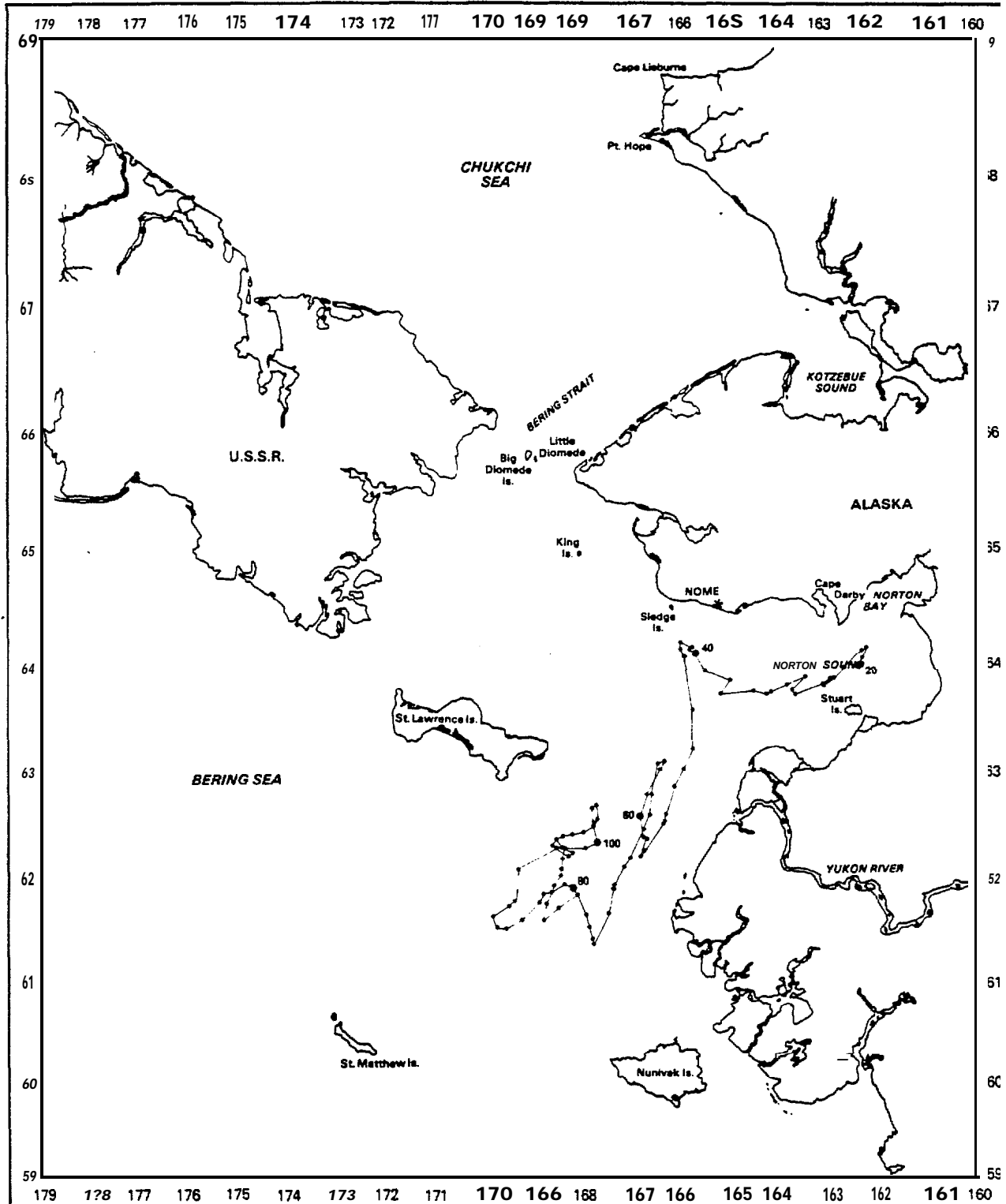


Figure 4. Trajectory of Buoy 3601 from January 20 to April 29, 1981 (Days 20 to 119). Daily Positions at 0000 Hours GMT Are Marked with Dots and Julian Days at 20-day Intervals Are Identified.

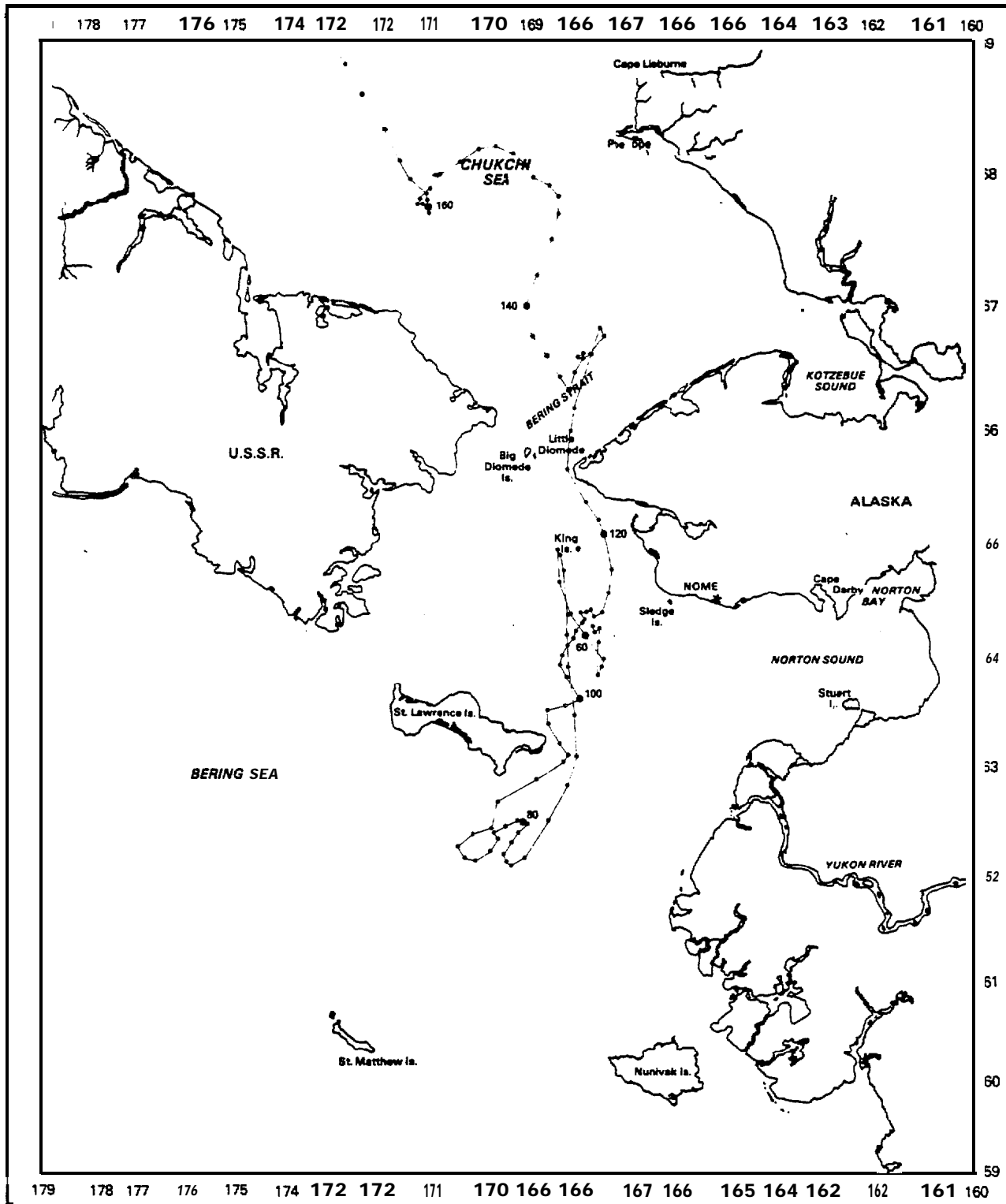


Figure 5. Trajectory of Buoy 3603 from February 21 to June 19, 1981 (Days 52 to 169). Daily Positions at 0000 Hours GMT Are Marked with Dots and Julian Days at 20-day Intervals Are Identified.

-14-

St. Lawrence Island. It then reversed its course again and consistently moved northward from that time until it ceased functioning on day 169. This buoy traveled through the Bering Strait and was continuing northward through the Chukchi Sea when it ceased reporting at 69 degrees north latitude.

In Figure 6 we present the motion of buoy 3605, which was deployed in the eastern portion of Norton Sound north of Stuart Island on Julian day 51. This buoy reported its position through day 91. Its general motion was toward the west out of Norton Sound during the first 20 days. After that it moved northward along the coast of Alaska until it ceased operation.

In Figure 7 we present the motion of buoy 3604, which was deployed just southwest of Nome on Julian day 75. This buoy reported its position through day 143. During this time period the buoy moved generally northwestward along the Alaskan coast. From day 94 through 129 the buoy appeared to be grounded near Point Spencer. After resuming its motion, it moved westward and later northward toward the Bering Strait. This buoy ceased reporting its position near Big Diomedes Island while drifting north through the Bering Strait.

In Figure 8 we present the motion of buoy 3606, which was deployed in the southern portion of Norton Sound on Julian day 75. This buoy reported its position through day 135. Its initial motion was westward out of the sound, after which it began to move to the south until approximately day 90 when it reversed its course. From approximately day 100 until a few days before it ceased operation, the buoy moved back and forth along the Alaskan coast near Sledge Island.

Buoys 3604 and 3606 again provide ice drift data showing strong spatial coherence with the other buoys. From roughly day 90 until ceasing operation, both buoys show a strong northward motion consistent with four of the other five buoys (only buoy 3600 traveled westward at the end of its course).

Buoys 3600 and 3603 were located on thick ice floes. These floes were thicker than 1 m and larger than 1 km in diameter. These two buoys survived longer and traveled further than the other five buoys. The remaining buoys were deployed on much thinner ice floes, in some cases as thin as 20 cm thick. Melting of the ice floes on which the buoys were stationed probably accounted for the end of transmission of all buoys except buoy 3605, which ceased operation near Big Diomedes Island while drifting north through the Bering Strait. It is easy to imagine that ice deformation would explain its demise.

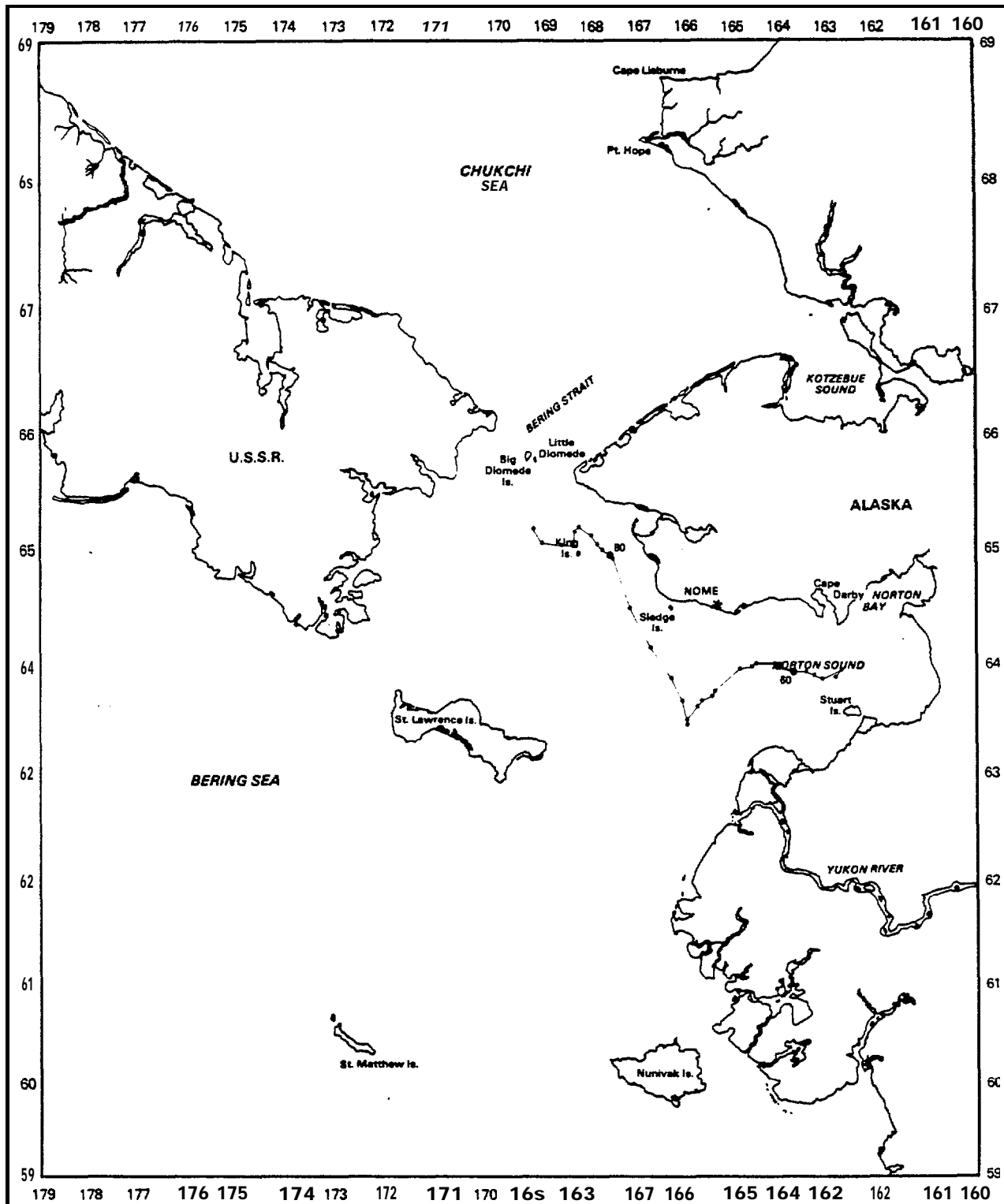


Figure 6. Trajectory of Buoy 3605 from February 20 to April 1, 1981 (Days 51 to 91). Daily Positions at 0000Hours GMT Are Marked with Dots and Julian Days at 20-day Intervals Are Identified.

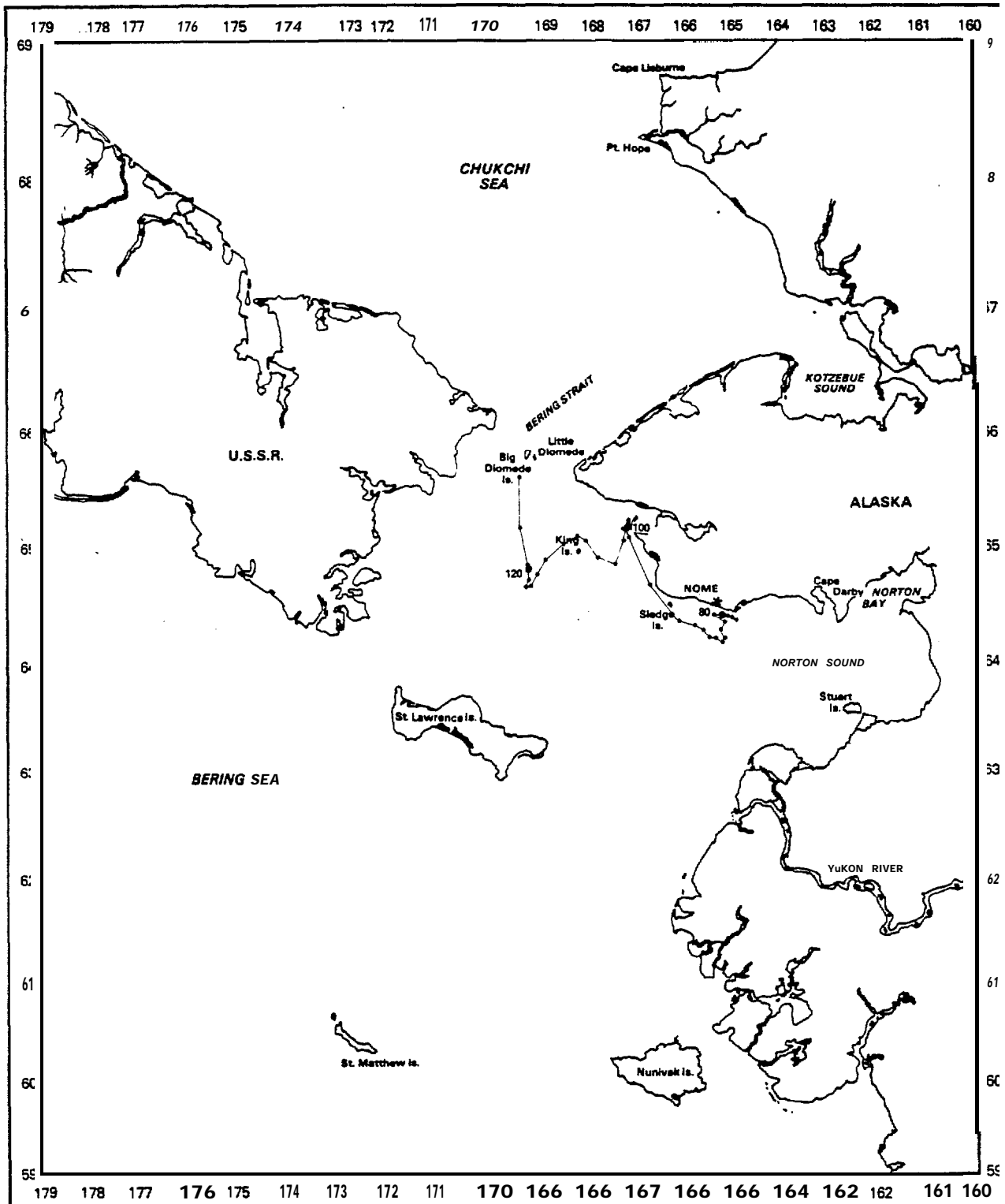


Figure 7. Trajectory of Buoy 3604 from March 16 to May 23, 1981 (Days 75 to 143). Daily Positions at 0000 Hours GMT Are Marked with Dots and Julian Days at 20-day Intervals Are Identified.

- 17 -

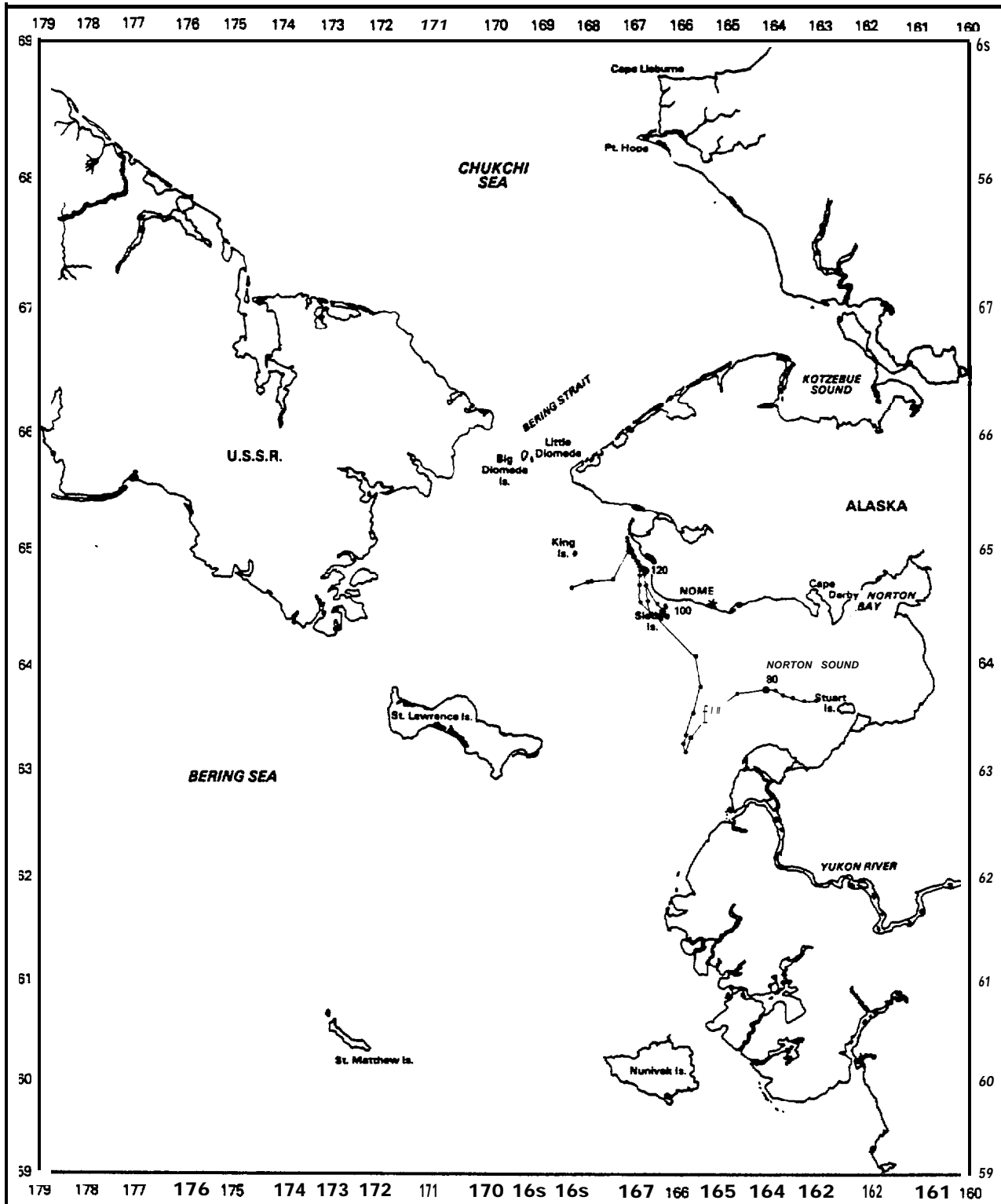


Figure 8. Trajectory of Buoy 3606 from March 16 to May 15, 1981 (Days 75 to 135). Daily Positions at 0000 Hours GMT Are Marked with Dots and Julian Days at 20-day Intervals Are Identified.

4.2 Discussion

The ice inside Norton Sound showed a consistent westward trend to its motion. Inside the sound, motions toward the north, south or east were limited in extent and always reversed within 2 or 3 days.

Between Norton Sound and St. Lawrence Island, the ice alternately moved south and north for several days at a time. Between days 43 and 56, the ice in this area moved south. **Between** days 57 and 62, the ice reversed and moved north. It then reversed again on day 63 and continuously moved south through day 72. Buoy 3600, which traveled farthest to the west, tended to move more toward the southwest during this last period, acquiring a more westerly motion as it passed beyond St. Lawrence Island. Buoy 3603, which traveled farthest to the north, tended to move more consistently **to the north as it neared the Bering Strait**. However, when moving southward, it traveled at nearly twice the speed of the other buoys. Buoy 3604 also picked up speed and moved more toward the north as it neared the strait. These alternating periods of north then south motions continued throughout the ice season in this region. The accumulated motion, however, was to the south.

Most buoys remained in constant motion. However, buoy 3604 did remain **motionless** during a 5-week period when it appeared to be with shorefast and grounded ice near Point Spencer. The buoy was very near some shoals only 3 m deep.

5. Conclusions

Several general features of the motion of sea ice in the Norton Sound area can be observed from the results of this study. First, during the period of this deployment program, the ice constantly moved westward out of Norton Sound. This implies a production of ice in the eastern portion of Norton Sound. Second, as the ice left the sound, the general trend was toward the southwest. This motion turned westward in the southern Bering Sea beyond St. Lawrence Island. **Third, substantial** reversals in the motion of the ice cover did occur. We do not know if these periods of northward motion are due to winds from the south or if they occur during periods of little wind when the northward currents dominate ice motions. In the vicinity of the Bering Strait, the strong northward currents through the strait seem to be a factor in ice motion. We do not know if a current reversal occurred in the Bering Strait during the course of this experiment. No buoys were near the strait during the periods of large ice motions toward the south. A reversal may have occurred during some of the periods of strong southward motion, such as during the period from days 64 through 73.

At this time we can only conjecture as to the relative importance of winds and ocean currents **at driving the sea ice** cover of Norton Sound and the Bering Sea. We doubt that **internal** ice stress plays a major role **in effecting ice** motions on **this spatial** scale. Of course, as one focuses closer to shore or on smaller scales, we must change this conclusion and recognize the fact that internal ice stress becomes the single most important factor. However, the large-scale motion of the ice cover is expected to satisfy a free-drift balance of forces. For the free-drift case, it is quite simple to correlate wind histories and ocean current histories with observed ice motion after processing winds and ocean currents through a free-drift model. This approach would allow a reasonable determination of the relative effects of winds and ocean currents on observed **motions**.

6. References

- Coachman, L. K., and Aagaard, K. (1981) "**Re-Evaluation** of Water Transports in the Vicinity of Bering Strait," in The Eastern Bering Sea Shelf - Oceanography and Resources, Vol. 1, ed. D. W. Hood and J. A. Calder, U.S. Dept. of Commerce, National Oceanic and Atmospheric Administration, Office of Marine Pollution Assessment, Juneau, Alaska, pp. 95-110.
- Kovacs, A. (1981) "Sea Ice Rubble Formations Off the Northeast Bering Sea and Norton Sound Coasts of Alaska," to appear in POAC 81, Vol. III.
- McNutt, L. (1981) Ice Conditions in the Eastern Bering Sea from NOAA and LANDSAT Imagery: Winter Conditions 1974, 1976, 1977, 1979, NOAA Technical Memorandum ERL PMEL-24.
- McPhee, M. G. (1980) "An Analysis of Pack Ice Drift in Summer," in Sea Ice Processes and Models, ed. R. S. Pritchard, University of Washington Press, Seattle, Washington, pp. 62-75.
- Pease, C. (1980) "Eastern Bering Sea Ice Processes," Monthly Weather Rev. 108, Vol. 12, pp. 2015-2023.
- Reimer, R. W., Schedvin, J. C., and Pritchard, R. S. (1981) "Chukchi Sea Ice Motion," in POAC 81, Vol. II, pp. 1038-1046
- Stringer, W. J. (1980) Nearshore Ice Characteristics in the Eastern Bering Sea, University of Alaska Geophysical Institute Report UAGR No. 278.
- Thorndike, A. S., and Colony, R. (1980) "Arctic Ocean Buoy Program Data Report 19 January 1979 to 31 December 1979," Published by the Polar Science Center, University of Washington, Seattle, Washington.

Appendix: Buoy Position Data

The smoothed daily positions and average daily velocities for buoys 3600 through 3606 are listed on the following pages. The first column gives the Julian day (with January 1, 1981, as day 1) and the second column gives the date at 0000 hours Greenwich Mean Time (GMT). The next two columns provide the positions in degrees latitude (north) and degrees **longitude** (west) at 0000 hours GMT, and the two final columns give the average velocity components at 1200 hours GMT (with positive velocities toward the north and the west).

-22-

BUOY ID NUMBER 3600

DAY	DATE	POSITION		VELOCITY(KM/DAY)	
		LAT(N)	LONG(W)	S-N	E-W
18	JAN 18	63.567	165.530	-20.3	-10.8
19	JAN 19	63.384	165.313	-15.8	-6.9
20	JAN 20	63.242	163. 175	-1.0	-3.4
21	JAN 21	63.233	16S.107	S.4	-3. 1
22	JAN 22	63.2S2	165.04S	5.9	4.5
23	JAN 23	63.335	165. 136	-20.0	8.8
24	JAN 24	63. 155	165.313	-18.2	6.7
25	JAN 25	62.991	165.447	9 . 9	1.4
26	JAN 26	63.080	165.475	33.3	-1 0 . 8
27	JAN 27	63.380	165.260	12.3	-6.9
28	JAN 28	63.491	165. 121	-7.8	4.3
29	JAN 29	63.421	165.208	-20.2	18.6
30	JAN 30	63. 167	165.580	26.8	-1.5
31	JAN 31	63.408	165.550	42.4	-13.4
32	FEB 1	63.790	165.279	-3.0	16.4
33	FEB 2	63.756	165.613	-32.0	8.3
34	FEB 3	63.468	165.7S2	-25.4	0.4
35	FEB 4	63.239	165.790	-17.2	9.0
36	FEB 5	63.004	165.969	-10.0	21.9
37	FEB 6	62.994	166.403	33.3	-e. 9
38	FEB 7	63.294	166.226	7.0	7.4
39	FEB 8	63.357	166.375	24. 1	2.7
40	FEB 9	63.574	166.430	12.5	0.2
41	FEB 10	63.687	166.43S	3.3	-4.2
42	FEB 11	63.717	166.349	-1.8	5.4
43	FEB 12	63.701	166.459	-7, 1	2.4
44	FEB 13	63.637	166.508	-18.7	1.8
45	FEB 14	63.469	166. 544	-34.9	5. 5
46	FEB 15	63. 155	166.633	-28.8	7.9
47	FEB 16	62.896	166.S12	-24. 1	9.9
48	FEB 17	62.679	147.006	-28.5	10. 1
49	FEB 18	62.422	167.203	-30.0	7.3
50	FEB 19	62. 152	167.344	-16.4	1.6
51	FEB 20	62.004	167.374	9.3	-1.4
52	FEB 21	62.007	167.348	-1.0	-3.3
53	FEB 22	61.998	167.284	-3.S	-2.8
54	FEB 23	61.964	167.230	-5.8	-1.3
55	FEB 24	61.912	167.204	-25,3	18.2
56	FEB 25	61.684	167.552	-3.9	10.2
57	FEB 26	61.649	167.745	8.4	-9.9
58	FEB 27	61.725	167.557	-2.1	5.8
59	FEB 28	61.706	167.668	23. 1	13.2
60	MAR 1	61.914	167.919	8.8	-5.6
61	MAR 2	61.993	167.812	21. 1	-7.5
62	MAR 3	62. 183	167.667	6.3	-3.0
63	MAR 4	62.240	167.609	-6.0	9.4
64	MAR 5	62. 186	167. 7'90	-29. 1	11.6
65	MAR '6	61.924	168.012	-22.7	10.0
66	MAR 7	61.720	168.203	1.0	8. 1
47	MAR '8	61.729	168.3S7	-12.4	10.7

BUOY ID NUMBER 3600

DAY	DATE	POSITION		VELOCITY(KM/DAY)	
		LAT(N)	LONG(W)	S - N	E - U
68	MAR 9	61.617	168.561	-26.1	21.4
69	MAR 10	61.382	168.965	-10.7	15.1
70	MAR 11	61.286	169.248	-17.7	18.8
71	MAR 12	61.127	169.599	-23.7	18.8
72	MAR 13	60.914	169.94S	-34.8	22.4
73	MAR 14	60.601	170.361	-13.4	15.0
74	MAR 15	60.480	170.635	-3.1	8.7
75	MAR 16	60.452	170.794	15.3	16.7
76	MAR 17	60.590	171.099	27.1	12.9
77	MAR 18	60.834	171.336	21.5	17.9
70	MAR 19	61.028	171.667	28.7	20.1
79	MAR 20	61.286	172.042	3.0	S.6
80	MAR 21	61.313	172.147	9.0	12.7
81	MAR 22	61.401	172.385	-1.9	14.9
82	MAR 23	61.384	172.665	-4.8	18.7
83	MAR 24	61.341	173.017	-1.8	9.1
84	MAR 25	61.325	173.188	-6.0	17.5
as	MAR 26	61.271	173.516	-9.8	18.9
86	MAR 27	61.183	173.869	-15.3	20.8
07	MAR 28	61.043	174.256	-3.2	14.8
88	MAR 29	61.016	174.532	9.2	7.4
89	MAR 30	61.099	174.670	3.3	-11.7
90	MAR 31	61.129	174.451	4.7	8.5
91	APR 1	61.171	174.609	18.5	5.4
92	APR 2	61.338	174.711	-4.2	-27.9
93	APR 3	61.300	174.188	-7.1	-2.7
94	APR 4	61.236	174.137	0.6	7.8
95	APR 5	61.241	174.283	-0.8	18.0
96	APR 6	61.234	174.619	-10.9	8.5
97	APR 7	61.136	174.778	-0.2	-11.7
98	APR 8	61.134	174.559	8.3	-16.3
99	APR 9	151.209	174.255	15.7	-0.9
100	APR 10	61.350	174.239	23.0	16.0
101	APR 11	61.557	174.540	15.2	2.9
102	APR 12	61.694	174.594	2.1	0.1
103	APR 13	61.713	174.596	1.1	7.8
104	APR 14	61.723	174.745	2.4	11.5
105	APR 15	61.745	174.963	1.4	10.8
106	APR 16	61.758	175.169	1.1	16.1
107	APR 17	61.768	175.473	-1.2	8.8
108	APR 18	61.757	175.642	-2.8	11.9
109	APR 19	61.732	175.569	-11.9	19.0
110	APR 20	61.625	176.229	-11.5	14.3
111	APR 21	61.521	176.500	-5.6	1.3
112	APR 22	61.471	176.525	4.7	-3.8
113	APR 23	61.513	176.453	2.6	-1.3
114	APR 24	61.536	176.42a	0.3	6.1
115	APR 25	61.539	176.543	-1.0	3.6
116	APR 26	61.530	176.611	13.5	-4.4
117	APR 27	61.6S2	176.527	19.0	-13.0

-24-

BUOY ID NUMBER 3600

DAY	DATE	POSITION		VELOCITY(KM/DAY)	
		LAT(N)	LONG(W)	S-N	E-U
118	APR 28	61.823	176.200	9.1	-18.4
119	APR 29	61.905	173.929	23.0	-19.8
120	APR 30	62.112	175.549	2.1	-10.9
121	MAY 1	62.131	175.339	6.4	-5.1
122	MAY 2	62.189	175.240	11.4	-5.7
123	MAY 3	62.292	175.130	-0.8	-0.7
124	MAY 4	62.28S	175.116	-11.1	0.2
125	MAY 5	62.185	175.120	0.3	-6.0
125	MAY 6	62.188	175.004	24.3	-7.2
127	MAY 7	62.407	174.865	22.2	0.5
128	MAY 8	62.607	174.874	2.0	5.4
129	MAY 9	62.625	174.979	-12.3	5.3
130	MAY 10	62.514	175.053	-8.6	7.2
131	MAY 11	62.437	175.263	-1.1	21.1
132	MAY 12	62.427	175.673	-0.2	2.0
133	MAY 13	62.425	175.711	-1.0	-9.7
134	MAY 14	62.416	175.522	5.6	11.3
135	MAY 15	62.466	175.742	-1.9	24.8
136	MAY 16	62.449	176.225	-1.8	14.2
137	MAY 17	62.433	176.502	-1.8	17.2
139	MAY 18	62.417	176.836	-2.7	24.2
139	MAY 19	62.393	177.306	-7.2	21.1
140	MAY 20	62.320	177.716	-6.0	23.4
141	MAY 21	62.274	178.16?	-17.2	26.4
142	MAY 22	62.119	178.67?	3.6	-2.7
143	MAY 23	62.151	178.527		

-25-

BUOY ID NUMBER 3601

DAY	DATE	POSITION		VELOCITY(KM/DAY)	
		LAT(N)	LONG(W)	S-N	E-W
20	JAN 20	64.017	162.378	7.0	-3.3
21	JAN 21	64.080	162.311	10.3	-3.5
22	JAN 22	64.173	162.238	-2.7	3.8
23	JAN 23	64.149	162.317	-18.5	17.1
24	JAN 24	63.982	162.669	-9.8	10.1
29	JAN 25	63.894	162.877	-8.4	10.9
26	JAN 26	63.818	163.100	6.3	-4.6
27	JAN 27	63.875	163.006	0.9	-3.7
20	JAN 28	63.883	162.931	-6.4	9.9
2?	JAN 29	63.82S	163.133	-9.8	28.3
30	JAN 30	63.737	163.709	4.4	1.9
31	JAN 31	63.777	163.748	13.7	-13.5
32	FEB 1	63.900	163.473	-8.1	18.7
33	FEB 2	63.S27	163.85S	-7.6	14.4
34	FEB 3	63.7S9	164.148	-1.6	5.5
3s	FEB 4	63.74S	164.259	2.2	13.4
36	FEE 5	63.76S	164.S32	-3.9	32.3
37	FEB 6	63.730	165.190	15.0	-8.7
38	FEB 7	63.865	163.012	10.1	24.6
39	FEB 8	63.956	165.516	15.7	9.7
40	FEB 9	64.097	165.716	5.0	5.0
41	FEB 10	64.142	165.S19	1.3	-3.9
42	FEB 11	64.154	165.738	4.8	13.3
43	FEB 12	64.197	166.012	-6.0	-0.1
44	FEB 13	64.143	166.010	-7.4	-2.4
45	FEB 14	64.076	165.960	-53.5	-9.0
46	FEB 15	63.594	165.776	-40.1	-0.8
47	FEB 16	63.233	165.760	-21.3	9.7
48	FEB 17	63.041	165.953	-23.8	10.2
49	FEB 18	62.827	166.154	-24.0	8.0
so	FEB 19	62.611	166.311	-11.3	3.5
51	FEB 20	62.509	166.379	2.4	-0.8
52	FEB 21	62.531	166.363	0.1	-0.6
53	FEB 22	62.532	166.351	-0.7	1.0
54	FEB 23	62.526	166.370	-1.8	0.8
55	FEB 24	62.510	166.385	-2s.0	19.0
56	FEB 2S	62.238	166.734	-s.0	3.7
97	FEB 26	62.213	166.825	20.3	-6.2
58	FEB 27	62.390	166.704	-0.7	3.6
59	FEB 28	62.3?2	166.773	21.0	2.6
60	MAR 1	62.581	166.823	23.3	-6.5
61	MAR 2	62.751	166.696	27.3	-12.8
62	MAR 3	63.037	166.442	9.0	-4.1
63	MAR 4	63.118	166.361	-3.2	4.9
64	MAR 5	63.089	166.459	-30.9	8.5
65	MAR 6	62.811	166.628	-24.0	2.7
66	MAR 7	62.595	166.682	3.8	-1.8
67	MAR- S	62.629	166.646	-14.2	6.0
68	MAR 9	62.501	166.764	-32.2	13.2
69	MAR- 10	62.211	167.020	-10.1	7.3

BUOY ID NUMBER 3601

DAY	DATE	POSITION		VELOCITY(KM/DAY)	
		LAT(N)	LONG(W)	S-N	E-W
70	MAR 11	62. 120	167.160	-21.0	10.4
71	MAR 12	61. 931	167.359	-30.0	5.2
72	MAR 13	61. 661	167. 459	-32.6	19.2
73	MAR 14	61. 367	167. 746	0.4	2.6
74	MAR 15	61. 371	167. 795	4. 8	-1.0
75	MAR 16	61.414	167.777	13.0	4. 1
76	MAR 17	61. 531	167.854	14.1	3.2
77	MAR 18	61. 658	167. 915	10.2	S.5
70	MAR 19	61.750	168.020	16.2	7. 5
79	MAR 20	61. 896	168.163	2. 1	2.3
80	MAR 21	61. 915	168.207	2.7	8.0
81	MAR 22	61.939	168.360	-0.2	12. 3
02	MAR 23	61. 865	168. 596	-0. 9	10.2
83	MAR 24	61.057	168. 791	-3.3	-0.5
84	MAR 25	61.827	168.782	-8.1	5.2
85	MAR 26	61. 754	168.881	-18. 1	18.1
86	MAR 27	61. 591	169.22S	-9.0	15. 7
87	MAR 28	61. 510	169.S22	1.0	11.0
88	MAR 29	61. 519	169,730	11. 5	3.S
89	MAR 30	61.623	169.802	11. 5	-16.S
90	MAR 31	61. 727	169. 483	6.6	-6.0
91	APR 1	61.786	149.369	34.5	-3.0
92	APR 2	62.097	169.297	23.7	-37.3
93	APR 3	62.310	168. 576	-6.0	-19. 5
94	APR 4	62. 256	168. 199	-3.2	3.4
9s	APR 5	62.227	168.265	5.4	11. 6
96	APR 6	62.276	168.489	6.2	5. 9
97	APR 7	62. 332	168.603	-3.9	-13.7
98	APR 8	62.297	168.338	-0.8	-20.0
99	APR 9	62.290	167.9S1	6. 1	-11.9
100	APR 10	62.345	167.721	20.2	3. 0
101	APR 11	62.S27	167.700	16. 7	2.3
102	APR 12	62.677	167.825	3.0	-3.0
103	APR 13	62.704	167.751	-16.1	-2.1
104	APR 14	62.559	167.710	-6.S	3.8
105	APR 15	62.498	167.783	-5. 8	8.7
106	APR 16	62.446	167.954	-1. 6	13. 1
107	APR 17	62.432	168.209	-3. 1	9. 1
108	APR 18	62.404	168.386	-3.3	4.0
109	APR 19	62.374	168.480	-0.6	2.0
110	APR 20	62.369	168.518	-7. 1	-6. &
111	APR 21	62.305	168.390	-11.9	0. 1
112	APR 22	62.198	166.392	-11.S	1.2
113	APR 23	62. 094	166.415	-8.1	1.7
114	APR 24	62. 021	168.44S	-10.1	6.5
11s	APR 29	61.930	168. 573	-19. 2	7.2
116	APR 26	61.7S7	168. 710	-18. 1	2.8
117	APR 27	61.S94	168.763	12.9	-15.2
118	APR 28	61.710	168. 474	14.8	-20. 6
119	APR '29	61. 843	168. 081		

-27-

BUOY ID NUMBER 3602

DAY	DATE	POSITION		VELOCITY(KM/ DAY)	
		LAT(N)	LONG(W)	S-N	E-U
18	JAN 18	63.777	163.998	-6.1	-14.6
19	JAN 19	63.722	163.701	-0.1	17.0
20	JAN 20	63.721	163.336	6.9	-10.2
21	JAN 21	63.703	163.149	8.1	-5.6
22	JAN 22	63.856	163.034	-1.7	S.8
23	JAN 23	63.841	%63.1S3	-7.1	18.7
24	JAN 24	63.777	163.534	-2.6	8.0
25	JAN 25	63.754	163.696	-1.9	14.1
26	JAN 26	63.737	163.984	7.4	-4.2
27	JAN 27	63.004	163.899	2.4	-1.5
28	JAN 28	63.826	163.868	-1.4	11.0
29	JAN 29	63.813	164.093	-6.7	32.6
30	JAN 30	63.753	164.757	0.6	-1.9
31	JAN 31	63.830	164.718	16.1	-10.8
32	FEB 1	63,975	164.497	-3.0	16.6
33	FEB 2	63.948	164.837	-24.3	20.7
34	FEE 3	63.729	16S.260	-9.7	1.7
35	FEB 4	63.642	165.294	-11.1	9.8
36	FEB 5	63.542	165.492	-22.5	15.8
37	FEB 6	63.339	165.810	29.9	-0.6
38	FEB 7	63.608	165,797	9.0	14.1
39	FEB 8	63.689	166.084	22.5	8.6
40	FEB 9	63.092	166.260	13.3	6.9
41	FEB 10	64.012	166.402	3.8	-1.6
42	FEB 11	64.046	166.370	1.3	9.1
43	FEB 12	64.058	166.557	-3.3	1.2
44	FEB 13	64.02S	166.5S2	-15.3	-3.8
45	FEB 14	63.890	166.504	-38.0	-5.3
46	FEB 15	63.548	166.397	-29.0	1.5
47	FEB 16	63.287	166.427	-22.1	7.9
48	FEB 17	63.088	166.585	-26.2	9.1'
49	FEB 18	62.852	166.766	-29.5	10.6
30	FEB 19	62.586	166.974	-16.5	6.4
51	FEB 20	62.437	167.098	2.1	-0.3
52	FEB 21	62.456	167.092	1.8	-2.7
53	FEB 22	62.472	167.040	0.6	-2.3
54	FEB 23	62.477	166.995	-2.6	-1.6
55	FEB 24	62.454	166.963	-27.5	11.9
56	FEB 29	62.206	167,194	-10.8	8.2
57	FEB 26	62.109	167.352	16.9	-9.8
58	FEB 27	62.261	167.162	-2.1	1.5
59	FEB 28	62.242	167.191	22.7	5.2
60	MAR 1	62.446	167.292	21.9	-7.6
61	MAR 2	62,643	167.143	35.0	-14.2
62	MAR 3	62.958	166.864	14.0	-4.7
63	MAR 4	63.084	166.770	-3.2	4.8
64	MAR 5	63.055	166.866	-32.1	9.1
65	MAR 6	62.766	167.026	-31.5	6.2
66	MAR 7	62.482	167.147	5.6	4.5
67	MAR 8	62.932	167.234	-13.3	6.5

BUOY ID NUMBER **3602**

DAY	DATE	POSITION		VELOCITY(KM/DAY)	
		LAT(N)	LONG(W)	S-N	E-U
68	MAR 9	62.412	167.361	-35.6	13.1
69	MAR 10	62.0?1	167.614	-14.3	7.2
70	MAR 11	61.962	167.752	-22.4	14.1
71	MAR 12	61.760	168.022	-29.0	12.8
72	MAR 13	61.499	168.265	-35.1	19.2
73	MAR 14	61.183	160.626	-6.3	8.1
74	MAR 15	61.126	168.777	1.0	0.4
7s	MAR 16	61.135	168.784	15.8	9.8
76	MAR 17	61.277	168.967	16.9	2.8
77	MAR 18	61.429	169.019	9.3	4.0
78	MAR 19	61.513	16?.095	16.0	8.1
79	MAR 20	61.657	169.249	1.3	2.2
80	MAR 21	61.669	169.290	0.9	5.9
81	MAR 22	61.677	169.402	-11.1	13.4
02	MAR 23	61.577	169.6S6	-5.9	11.0
83	MAR 24	61.524	169.864	-4.3	5.8
84	MAR 25	61.485	169.973	-S.4	12.0
85	MAR 26	61.436	170.199	-18.3	31.1
86	MAR 27	61.271	170.784	-10.8	20.3
87	MAR 28	61.174	171.164	6.0	14.2
88	MAR 29	61.235	171.430	14.5	5.5
89	MAR 30	61.366	171.534	11.8	-19.0
90	MAR 31	61.472	171.176	11.7	0.3
91	APR 1	61.577	171.182	37.3	1.7
92	APR 2	61.913	171.214	18.4	-35,2
93	APR 3	62.079	170.538	-4.4	-18.9
94	APR 4	62.039	170.175	2.2	4.7
95	APR 5	62.059	170.266	4.0	16.3
96	APR 6	62.095	170.579	5.1	9.9
97	APR 7	62.141	170.770	-0.4	-13.0
90	APR 8	62.137	170.519	3.3	-20.9
99	APR 9	62.167	170.117	11.0	-9.7
100	APR 10	62.266	169.930	22.4	6.5
101	APR 11	62.46a	170.056	21.0	5.0
102	APR 12	62.6S7	170.153	1.6	-13.1
103	APR 13	62.671	169.896	-7.2	-14.2
104	APR 14	62.606	169.617	-0.3	0.2
10s	APR 15	62.603	169.621	-o. 1	7.s
106	APR 16	62.602	169.767	-1.2	13.4
107	APR 17	62.S91	170.029	-3.8	12.4
108	APR 18	62.557	170.271	-3.3	10.9
109	APR 19	62.S27	170.4S3	-3.3	18.2
110	APR 20	62.497	170.038	0. 1	5.6
111	APR 21	62.490	170.947	-5.9	-4, 8
112	APR 22	62.44S	170.054	-8.3	0.1
113	APR 23	62.370	170.855	-6.4	4.3
114	APR 24	62.312	170.938	-S. 6	5.9
115	APR 25	62.235	171.0S3	-17.3	1.0
116	APR 26	62.079	171.087	-6.0	-7.0
117	APR 27	62.025	170.938	16.8	-20.2

-29-

BUOY ID NUMBER 3602

DAY	DATE	POSITION		VELOCITY(KM/DAY)	
		LAT(N)	LONG(W)	S-N	E-W
118	APR 2S	62. 176	170.s49	11.5	-20.6
119	APR 29	62.280	170.150	15. 2	-31.2 .
120	APR 30	62. 417	169. 544	2.2	-6. 9
121	HAY 1	&2.437	169.409	-2.1	-39. 7
122	MAY 2	62. 418	168. 637	17.4	-18. 2
123	MAY 3	62. 575	168.282	17.3	-12. 8
124	MAY 4	62.731	168.031	-6. 1	4."3
125	MAY 5	62. 676	168. 120	-24.1	-3.3
126	MAY 6	62. 459	168. 052	19. 8	-16.9
127	MAY 7	62. 637	167. 722	11. 4	-18. 0
12a	MAY 8	62.740	167. 368	10. 5	-2.4
129	MAY 9	62. 835	167.321	-10. 7	2.0
130	MAY 10	62. 739	167. 361		

-30-

BUOY ID NUMBER 3603

DAY	DATE	POSITION		VELOCITY(KM/DAY)	
		LAT(N)	LONG(W)	S-N	E-W
52	FEB 21	64.273	167.S25	-5.7	-3.S
53	FEB 22	64.222	167.752	4. 1	-2.7
54	FEB 23	64.259	167.697	0.6	0.S
5s	FEB 24	64.264	167.708	-12. 1	1.0
56	FEB 2S	64. 1S5	167.728	-32. 5	-2.7
57	FEE 26	63.862	167.673	11. 3	-1.7
58	FEB 27	63. 964	167.638	7. 1	0.2
59	FEB 28	64.028	167.643	19. 4	14.4
60	MAR 1	64.203	167.941	20.S	15. 4
61	MAR 2	64. 388	16S.261	31. 2	7. 8
62	MAR 3	64.669	160.424	30.8	0.6
63	MAR 4	64.946	168. 436	4.6	0. 6
64	MAR 5	64.987	168.449	-22.4	-2. 6
6s	MAR 6	64. 785	168.393	-44.9	-4.3
66	MAR 7	64.381	168.302	-24.0	0.3
67	MAR 8	64. 165	168.309	-26.5	-1. 3
68	MAR 9	63.926	16S.283	-49.4	-6.2
69	MAR 10	63.481	168. 156	-41.6	-2.1
70	MAR 11	63. 106	168.113	-29. 1	10.3
71	MAR 12	62.844	168.318	-38. 1	19. 4
72	MAR 13	62.501	168. 698	-37.8	26.4
73	MAR 14	62. 161	169.209	-7.7	13.3
74	MAR 15	62.092	169.466	2.2	5.3
7s	MAR 16	62. 112	169.560	10.5	1.3
76	MAR 17	62.207	169.394	12.9	-7.9
77	MAR 18	62.323	169.442	9.0	-7.4
78	MAR 19	62.404	169.295	7.8	-e. s
79	MAR 20	62.474	169. 130	1. 1	1.5
so	MAR 21	62.484	169. 160	2.8	8.8
81	MAR 22	62.509	169.331	-6.8	11. 5
82	MAR 23	62.448	169. 555	-5.2	14.2
83	MAR 24	62. 401	169.031	-0.2	-2.4
04	MAR 25	62. 399	169.784	-6. 1	-3.3
85	MAR 26	62.344	169. 719	-12.9	8. 1
86	tlAR 27	62.228	169. 876	-0.9	15.2
87	MAR 28	62. 148	170. 170	2.3	11. 5
08	MAR 29	62. 169	170,392	11. 5	7.9
89	MAR 30	62.273	170. 545	14. 0	-16.4
90	MAR 31	62.399	170.227	5.8	-19.6
91	APR 1	62. 451	169. 845	27.2	-6.9
92	APR 2	62.696	169.711	22.9	-40. 0
93	APR 3	62.902	168.923	16. 5	-28.0
94	APR 4	63.051	168.369	7.7	-3.3
9s	APR 5	63. 120	168. 304	11.3	7.8
96	APR 6	63.224	168.460	19. 9	11. 4
97	APR 7	63.403	168.608	14.8	1.7
98	APR 8	63.536	168.722	3. 1	-21.2
99	APR 9	63. 564	168.294	S.9	-8.6
100	APR 10	63. 617	168.120	17. 4	6.7
101	APR 11	63.774	168. 257	17.9	9.7

-31-

BUOY ID NUMBER 3603

DAY	DATE	POSITION		VELOCITY(KM/DAY)	
		LAT(N)	LONG(W)	S-N	E-W
102	APR 12	63.935	168.453	10.4	-2.8
103	APR 13	64.029	168.398	7.6	-5.3
104	APR 14	64.097	160.289	9.0	-s. 2
105	APR 15	64.178	168.182	7.2	-3.6
106	APR 16	64.243	168.107	4.1	-4.2
107	APR 17	64.280	160.020	3.7	-2.4
108	APR 18	64.313	167.970	4.8	-1.9
109	APR 19	64.356	167.931	2.6	2.9
110	APR 20	64.379	167.992	2.4	1.7
111	APR 21	64.401	168.027	-0.6	-0.6
112	APR 22	64.396	168.013	0.9	-3.7
113	APR 23	64.404	167.938	3.0	-4.0
114	APR 24	64.431	167.8S9	-0.8	-1.4
115	APR 25	64.424	167.826	-5.6	-4.7
116	APR 26	64.374	167.729	0.2	-7.4
117	APR 27	64.376	167.374	21.5	-5.7
118	APR 28	64.570	167.454	23.5	-3.1
119	APR 29	64.782	167.388	36.3	6.3
120	APR 30	65.109	167.521	11.4	6.3
121	MAY 1	65.212	167.656	17.3	10.6
122	MAY 2	65.368	167.804	31.2	17.8
123	MAY 3	65.649	168.271	38.1	-3.0
124	MAY 4	6S.992	168.205	-2.3	0.8
125	MAY 5	65.971	168.222	22.0	-3.0
126	MAY 6	66.149	168.137	46.2	-16.7
127	MAY 7	66.585	167.762	21.7	-8.6
128	MAY 8	66.780	167.566	1.2	-0.5
129	MAY 9	66.791	167.554	-4.4	0.2
130	MAY 10	66.751	167.559	-17.0	8.8
131	MAY 11	66.598	167.760	-5.9	12.1
132	MAY 12	66.545	168.033	4.8	-4.1
133	MAY 13	66.588	167.941	-3.3	0.7
134	MAY 14	66.ss8	167.957	-13.0	7.8
135	MAY 15	66.441	168.134	-14.2	S.5
136	MAY 16	66.313	168.257	11.0	7.s
137	MAY 17	66.412	168.425	19.5	11.5
138	MAY 18	66.588	168.684	14.9	12.8
139	HAY 19	66.722	168,976	29.9	3.0
140	nAY 20	66.991	169.045	27.0	-7.7
141	MAY 21	67.234	168.866	30.3	-12.9
142	MAY 22	67.507	168.563	22.5	-6.3
143	MAY 23	67.710	168.415	15.0	0.9
144	MAY 24	67.843	168.436	8.9	7.0
145	MAY 25	67.925	168.604	7.2	14.9
146	MAY 26	67.990	168.961	12.3	7.0
147	MAY 27	68.101	169.130	7.8	9.4
148	MAY 28	68.171	169.358	6.0	13.0
149	MAY 29	68.225	169.672	-2.7	13.9
150	MAY 30	68.201	170.009	-10.S	17.7
151	JUN 1	68.106	170.437	-11.1	17.4

BUOY ID NUMBER 3603

DAY	DATE	POSITION		VELOCITY(KM/DAY)	
		LAT(N)	LONG(W)	S-N	E-w
152	JUN 2	68.006	170.857	-9.8	6.7
153	JUN 3	67.918	171.019	-3.7	2.9
134	JUN 4	67.885	171.079	-6.2	5.4
155	JUN 5	67.829	171.207	-4.4	1.8
156	JUN 6	67.789	171.291	0.7	0.5
157	JUN 7	67.795	171.262	1.0	-2.1
150	JUN 8	67.804	171.212	-8.8	-6.7
159	JUN 9	67.728	171.053	5.4	3.3
160	JUN 10	67.774	171.132	3.4	1.0
161	JUN 11	67.805	171.157	3.2	0.3
162	JUN 12	67.834	171.168	5.2	4.4
163	JUN 13	67.881	171.269	11.0	7.1
164	JUN 14	67.980	171.439	14.4	8.7
165	JUN 15	68.110	171.648	27.4	12.7
166	JUN 16	68.357	171.957	28a	17.0
167	JUN 17	68.616	172.374	23.8	14.7
168	JUN 18	68.830	172.739	14.9	7.0
169	JUN 19	68.964	172.915		

BUOY ID NUMBER 3604

DAY	DATE	POSITION		VELOCITY(KM/DAY)	
		LAT(N)	LONG(W)	S-N	E-U
7	5	MAR 16	64.363 164.886	3.3	2.2
76	MAR 17	64.393	164.931	2.1	5.0
77	MAR 18	64.412	16S.0S2	0.2	3.2
78	MAR 19	64.414	165.110	0.3	9.6
79	MAR 20	64.417	163.310	0.1	-0.4
80	MAR 21	64.410	16S.309	-6.0	-11.4
81	MAR 22	64.357	165.071	-7.7	5.1
02	MAR 23	64.288	165.176	-9.6	-4.5
83	MAR 24	64.202	163.082	-3.7	2.2
84	MAR 2S	64.149	165.127	3.9	5.2
85	MAR 26	64.204	163.23S	-0.1	2.3
86	MAR 27	64.203	165.203	-0.6	-0.8
87	MAR 28	64.198	16S.267	2.4	5.7
88	MAR 29	64.220	16S.386	6.2	6.5
89	MAR 30	64.281	165.521	4.3	7.4
90	MAR 31	64.320	165.674	5.1	16.3
91	APR 1	64.366	166.014	37.4	27.7
92	APR 2	64.703	166.595	45.S	20.5
93	APR 3	65.113	167.030	7.0	3.1
94	APR 4	65.176	167.097	-0.1	-0.2
95	APR S	65.175	167.093	0.0	0.0
96	APR 6	65.175	167.092	0.0	0.0
97	APR 7	6S.175	167.092	0.3	0.0
98	APR 8	65.178	167.092	1.2	-0.4
99	APR 9	6S.189	167.084	-0.1	0.6
100	APR 10	6S.188	167.096	-0.1	-0.6
101	APR 11	65.187	167.083	0.0	-0.2
102	APR 12	63.187	167.079	0.0	-0.2
103	APR 13	65.187	167.075	0.0	0.3
104	APR 14	65.187	167.081	0.7	0.6
105	APR 15	69.193	167.093	-0.2	-0.3
106	APR 16	65.191	167.086	-0.1	-0.1
107	APR 17	6S.199	167.083	0.0	-0.3
108	APR 18	65.190	167.077	0.0	0.2
109	APR 19	65.190	167.001	0.0	-0.1
110	APR 20	65.190	167.078	-0.1	0.0
111	APR 21	65.189	167.07S	0.1	0.1
112	APR 22	65.190	167.080	-0.1	0.0
\$13	APR 23	65.189	167.081	0.1	0.0
114	APR 24	65.190	167.080	-0.1	0.0
115	APR 2S	65.189	167.080	0.2	0.0
116	APR 26	65.191	167.080	0.0	-0.1
117	APR 27	65.191	167.078	-0.1	0.0
118	APR 28	65.190	167.079	-0.1	0.2
119	APR 29	65.189	167.084	0.2	0.0
120	APR 30	65.191	167.085	-0.1	-0.1
121	MAY 1	65.190	167.082	-0.1	-0.1
122	MAY 2	65.189	167.079	0.0	-0.1
123	MAY 3	65.189	167.077	0.0	0.1
124	MAY 4	65.189	167.080	0.0	0.1

BUOYID NUMBER 3604

DAY	DATE	POSITION		VELOCITY(KM/DAY)	
		LAT(N)	LONG(W)	S-N	E-W
12s	MAY 5	65.189	167.082	0.1	-0.1
126	MAY 6	65.190	167.080	0.1	0.0
127	MAY 7	65.191	167.079	-0.1	0.1
12s	MAY 8	6S.190	167.081	-0.1	9.0
129	MAY 9	63.189	167.080	0.0	-0.2
130	RAY 10	6S.189	167.076	-11.1	1.5
131	MAY 11	6S.089	167.108	-24.8	7.3
132	MAY 12	64.866	167.264	7.7	18.3
133	MAY 13	64.935	167.4S2	17.S	11.1
134	MAY 14	6S.093	167.889	-3.3	20.7
135	MAY 15	6S.063	168.331	-16.7	19.3
136	MAY 16	64.913	168.741	-11.2	6.4
137	MAY 17	64.812	168.877	-2.1	0.0
130	MAY 18	64.793	168.878	-10.S	6.0
139	MAY 19	64.698	169.00S	-1.9	4.2
140	MAY 20	64.681	169.094	20.1	-1.s
141	MAY 21	64.862	169.063	39.1	6.3
142	MAY 22	65.214	169.197	49.0	0.8
143	MAY 23	65.662	169.215		

BUOY ID NUMBER 3605

DAY	DATE	POSITION		VELOCITY(KM/DAY)	
		LAT(N)	LONG(W)	S - N	E - U
51	FEB 20	63.892	162.860	-0.9	1.2
52	FEB 21	63.884	162.885	3.2	-4.8
53	FEB 22	63.913	162.786	3.4	-2.8
94	FEB 23	63.945	162.720	-0.3	2.9
55	FEB 24	63.942	162.788	-9.1	17.2
56	FEB 29	63.860	163.140	2.2	9.0
57	FEB 26	63.880	163.323	2.8	-1.6
58	FEB 27	63.905	163.271	1.8	6.1
59	FEB 28	63.921	163.413	2.2	14.1
60	MAR 1	63.941	163.704	3.6	14.8
61	MAR 2	63.973	164.007	3.4	-6.3
62	MAR 3	64.004	163.878	0.4	2.8
63	MAR 4	64.008	163.936	0.6	7.2
64	MAR 5	64.013	164.084	-0.4	18.8
6s	MAR 6	64.009	164.471	-3.2	4.5
66	MAR 7	63.980	164.563	2.8	-1.4
67	MAR 8	64.005	164.534	-5.4	13.6
6a	MAR 9	63.956	164.813	-21.5	21.3
69	MAR 10	63.762	16S.248	-5.0	3.6
70	MAR 11	63.717	16S.321	-5.0	10.8
71	MAR 12	63.672	165.541	-6.3	5.7
72	MAR 13	63.615	163.6S7	-19.2	9.S
73.	MAR 14	63.442	16S.849	5.7	-0.2
74	MAR 15	63.493	165.845	18.8	5.8
7s	MAR 16	63.662	165.962	24.3	9.7
76	MAR 17	63.881	166.199	30.1	29.6
77	MAR 18	64.152	166.583	24.S	1S.2
78	MAR 19	64.373	166.898	63.9	21.6
79	MAR 20	64.948	167.353	2.6	1.9
00	MAR 21	64.971	167.394	6.6	8.3
81	MAR 22	69.030	167.570	5.0	3.6
82	MAR 23	65.075	167.647	0.6	1.8
83	MAR 24	65.080	167.685	10.2	5.9
84	MAR 2S	65.172	%67.812	7.4	10.6
85	MAR 26	65.239	168.039	-5.7	3.2
86	MAR 27	65.188	168.108	-10.8	0.7
87	MAR 28	65.091	168.124	-5.2	1.1
88	MAR 29	65.044	168.147	2.2	12.0
89	MAR 30	65.064	168,403	4.4	18.8
90	MAR 31	65.104	168.004	14.4	7.5
91	APR 1	65.234	168.964		

BUOY ID NUMBER 3604

DAY	DATE	POSITION		VELOCITY(KM/DAY)	
		LAT(N)	LONG(W)	S-N	E-W
7s	MAR 16	63.612	163.148	-1.8	13.4
76	MAR 17	63. S961	163.420	3.8	11.1
77	MAR 18	63.630"	163.644	2.2	9.8
78	MAR 19	63.650	163.843	8.2	10.2
79	MAR 20	63.724	164.051	-0.4	6.2
80	MAR 21	63.720	164.177	-5.7	29.7
81	MAR 22	63.669	164.781	-23.7	29.5
82	MAR 23	63.456	165.378	-21.5	16.1
83	MAR 24	63.262	165.701	-0.9	2.8
84	MAR 25	63.254	165.757	1.8	2.2
0s	MAR 26	63.270	165.801	-8.2	3.0
86	MAR 27	63.196	165.861	-8.0	-0.6
87	MAR 28	63.124	165.500	-2.2	-1.7
88	MAR 29	63.104	165.813	13.8	-0.7
09	MAR 30	63.228	165.500	28.8	-7.3
90	MAR 31	63.487	165.654	2a. 1	-7.3
91	APR 1	63.740	165.506	31.3	4.6
92	APR 2	64.022	165.600	30.8	22.4
93	APR 3	64.299	166.063	12.3	17.0
94	APR 4	64.410	166.416	-0.8	1.2
95	APR 5	64.403	166.442	0.1	1.6
96	APR 6	64.404	166.475	0.9	2.0
97	APR 7	64.412	146.516	-1.0	-10.4
90	APR 8	64.403	166.300	1.3	-4.1
99	APR 9	64.415	166.215	3.2	3.3
100	APR 10	64.444	166.284	6.0	3.2
101	APR 11	64.505	166.365	20.1	12.5
102	APR 12	64.686	166.620	10.8	1.3
103	APR 13	64.783	166.656	5.0	1.4
104	APR 14	64.828	166.685	0.4	1.0
105	APR 15	64.832	166.705	-0.3	-0.4
106	APR 16	64.029	166.697	0.3	0.6
107	APR 17	64.832	166.709	0.8	0.2
108	APR 18	64.839	166.713	1.0	0.3
109	APR 19	64.848	166.719	1.2	1.3
110	APR 20	64.859	166.747	5.2	2.8
111	APR 21	64.906	166.806	0.0	0.1
112	APR 22	64.906	166.808	-6.8	-2.4
113	APR 23	64.045	166.757	-7.3	-0.8
114	APR 24	64.779	166.740	-10.5	0.2
115	APR 25	64.684	166.745	-17.5	-1.5
116	APR 24	64.826	166.713	-13.8	-9.1
117	APR 27	64.402	166.522	14.9	2.3
118	APR 28	64.336	166.570	16.2	2.0
119	APR 29	64.682	166.629	13.2	0.6
120	APR 30	64.801	166.642	1.2	0.3
121	HAY 1	64.812	166.648	-0.2	0.0
122	MAY- 2	64.810	166.647	10.5	6.3
123	MAY 3	64.905	166.750	15.4	9.0
124	MAY- 4	63.044	166.971	-13.1	-4.6

-37-

BUOY ID NUMBER 3 6 0 6

DAY	DATE	POSITION		VELOCITY(KM/DAY)	
		LAT(N)	LONG(W)	S-N	E-W
125	MAY 5	64.926	166.873	-s. 3	-4.5
126	MAY 6	64.878	166.778		23.2
127	MAY 7	65.087	167.004	0.4	0.4
12s	MAY 8	65.091	167.013	0.1	-0.1
129	MAY 9	65.092	167.011	-0.2	-0.2
130	MAY 10	65.087	167.007	-12.0	-3.0
131	MAY 11	64.979	166.942	-27.9	16.4
132	MAY 12	64.728	167.289	-2.4	22.0
133	MAY 13	64.706	167.753	0.0	2.3
134	MAY 14	64.706	167.002	-5.1	15.1
135	MAY 15	64.660	168.121		

APPENDIX C
THE TURBULENT BOUNDARY LAYER IN SHALLOW WATER

Miles G. McPhee

29 January 1981

1. Introduction

This report addresses the behavior of turbulence driven currents in a shallow water column -- one in which the bottom plays a significant role in modifying the structure of turbulence and velocity in the boundary layer. The problem is difficult and the theory developed here should be considered exploratory, in part because there are few data with which to test its applicability.

The basic question asked is how the structure of the boundary layer is changed by the presence of a bottom surface. Specific applications include modification of the drag law (i.e., the relationship between surface (ice) velocity and interracial stress). The results show that, for the same stress, the ice motion may vary widely depending on the depth, even when complicating effects like nearshore pressure gradients are ignored.

The conditions under which the present approach is considered valid are quite restricted and should be kept in mind. First, the water column is taken to be well mixed throughout, so that turbulence is not inhibited by density gradients in the fluid. Data on water density over the shallower parts of the shelf in the Beaufort are limited, and highly biased toward summer sampling. By the end of summer, vertical stratification from melting ice and continental runoff is **trong** and there is a marked increase in the salinity of the surface layer from the shelf seaward. However, **Aagaard** (1981) points out that by late winter, this gradient has reversed, and it is plausible that well mixed conditions persist over much of the shelf for extensive periods during the fall. Garrison, **Welch**, and Shaw (1979) show profiles from the **Chukchi** in April where water of depths from 30-50 m is almost **isohaline**. As this is late in the freezing season, it also suggests that stratification is small during much of the year. According to Pease (1980), the water column in the eastern Bering is completely mixed when the depth is less than about 50 m.

The second major restriction in the present model is that the only forces acting on the fluid are turbulent stresses due only to frictional surface stress, i.e., stress transferred directly from the wind or through moving pack ice. There are problems here: when wind acts upon a shallow sea one can expect a response not tied directly to turbulent shear, because divergent transport will set up pressure gradients which act upon the entire water. Such effects are apparent during storm surges, which are abnormal changes in sea level caused by high winds. The intent is to consider what happens in the short term, so that for the most part we shall ignore sea level changes. The theory does, however, indicate some interesting consequences of the shallow boundary layer on mass divergence, which we shall explore briefly.

The work is an extension of the analytic planetary boundary layer (PBL) theory described by McPhee (1981), summarized as follows: (1) turbulent stress in the boundary layer responds to an eddy momentum **diffusivity** that is determined by the product of the friction velocity u_* (the square root of the kinematic interracial stress) times a maximum mixing length. (2) The maximum mixing **length** depends in a simple way on u_* and the surface buoyancy flux so that it is proportional to u_*/f in the neutral limit, and to the critical flux Richardson number when surface buoyancy is dominant. (3) Mean velocity responds to the same eddy viscosity except in a thin layer adjacent to the interface, which gives rise to a logarithmic-like layer near the surface. Strong surface buoyancy occurs when there is rapid melting, and can have a large impact on drag. Rapid melting is usually associated with strong stratification throughout the water column, which effectively isolates the surface from bottom friction. While the theory is equipped to deal with surface buoyancy, it is not considered important in this particular application.

2. Extension of the Theory

The shallow boundary-layer extension is best introduced by considering a "turbulent **Couette**" flow, i.e., one in which the separation between two bounding surfaces (which are moving relative to each other) is small enough that the turbulent stress in the bounded fluid is constant. In a **laminar** fluid with constant viscosity such a flow is characterized by constant shear and a linear mean velocity profile between the surfaces. In a turbulent flow, the eddy viscosity varies across the separation and the mean profile is more complicated; nevertheless, a rather simple solution can be found by applying straightforward turbulence principles. The mixing length is assumed to vary linearly from each surface, so that the effective eddy viscosity is $K=ku_*z$, where k is **Karman's** constant, u_* is the magnitude of the friction velocity and z is the distance from each surface, up to half of the total distance. The solution is sketched in Figure 1. Note that the size of the energy containing eddies is sensitive only to the distance from the surface, not the roughness. Therefore the maximum eddy size occurs at the mid-depth plane even though the mean velocity profile is symmetric only if the $z_{OT} = z_{OB}$.

Geophysical flows similar to that sketched in Figure 1 can be found (e.g., ice drifting relative to a shallow bottom), however, the scales are often such that the assumption of constant turbulent stress throughout the fluid is questionable. Consider, for example, the idealized, steady-state boundary layer in an infinitely deep fluid as depicted in Figure 2, from McPhee (1981). For convenience, the solutions are shown in nondimensional form: kinematic stress is **nondimensionalized** by u_*^2 , velocity by u_*/η_* , and depth by η_*u_*/f . η_* is a stability factor that is unity for neutrally stable surface conditions (the case being considered here) and f is the **Coriolis** parameter. A typical value for the neutral **length** scale, u_*/f , is around 70 m. From Figure 2, one can see that by about 10 m depth the stress in the bottomless boundary layer has lost half its magnitude and has also undergone a considerable rightward deflection. We can surmise from this that the effect of rotation will modify turbulence, even in relatively shallow waters. The thrust of the present work is to estimate the effect of rotation, and to provide a reasonable conceptual transition from the turbulent Couette flow studied in the laboratory to the developed rotational boundary layer found to exist under pack ice over the deep ocean.

The most important assumption in the shallow layer extension is that in calculating the turbulent stress, the eddy viscosity can be considered constant with depth and that Ekman dynamics govern the stress distribution. This assumption is clearly open to question, and deserves more attention, both in terms of actual measurements and theoretical development. For the present, consider it a working hypothesis.

From McPhee (1981), the nondimensional variables for the turbulent boundary layer are:

$$\begin{aligned} \text{Stress:} & \quad \hat{T} = \hat{\tau} / u_* \hat{u}_* \\ \text{Velocity:} & \quad \hat{v} = \eta_* \hat{U} / u_* \\ \text{Vertical Coordinate:} & \quad \zeta = fz / \eta_* u_* \\ \text{Eddy Viscosity:} & \quad K^* = fK / u_*^2 \eta_*^2 \end{aligned}$$

where u_* is the friction velocity (a vector) defined by $u_* \hat{e}_* \hat{\tau}_0$ when $\hat{\tau}_0$ is the kinematic stress at the upper interface; and η_* is a stability factor that depends on the rate of melting (or heating) at the surface -- unless otherwise noted the effects of surface buoyancy are neglected and $\eta_* = 1$. The interested reader is referred to McPhee (1981) for more detail on boundary-layer scaling and representation of two-dimensional vectors as complex numbers.

The steady-state, horizontally homogeneous, stress equation is given by

$$i\hat{T}/K_* = \frac{\partial^2 \hat{T}}{\partial \zeta^2}$$

with solution:

$$\hat{T} = \hat{A} (e^{\delta \zeta} - e^{-\delta \zeta}) + e^{\delta \zeta}$$

since $\hat{T}(0)=1$, and where $\delta = (i/K_*)^{1/2}$

The lower boundary condition in the Ekman solution is

$$\hat{v}(\zeta_m) = \frac{1}{K_*} \frac{\partial \hat{T}}{\partial \zeta} \Big|_{\zeta_m} = 0 \text{ at } \zeta_m = fz_{\text{bot}} / u_* \eta_*$$

from which

$$\hat{A} = e^{-\delta \zeta_m} (e^{\delta \zeta_m} + e^{-\delta \zeta_m})$$

and

$$\hat{T}_b = \hat{T}(\zeta_m) = e^{-\delta \zeta_m} [\tanh(\delta \zeta_m) - 1]$$

This provides a relatively simple analytic expression for the stress distribution in terms of complex exponential.

By analogy with the approach taken for the open ocean boundary layer (McPhee, 1981), the mean velocity profile is considered in sections, in this case, three zones: a logarithmic bottom surface layer, an interior Ekman layer, and a near surface log-linear layer. Figure 3 is a schematic of the system, but is somewhat misleading in that the velocity profile rotates about a vertical axis. The mathematical description of the mean velocity **is** developed as follows. Consider first the bottom surface layer (recall that the stress solution does not depend on variation of eddy viscosity in the surface layers): the thickness of the layer depends on the local friction velocity and is given in nondimensional coordinates by $\Delta\zeta = T_b^{1/2} \xi_N$. The nondimensional equation for shear **is**

$$(k/\eta_*) (\zeta - \zeta_m) T_b^{1/2} \frac{\partial \hat{v}}{\partial \zeta} = T(\zeta) = T_b + \frac{(\zeta - \zeta_m)}{T_b^{1/2} \xi_N} (T_{bsl} - \hat{T}_b)$$

'here' $\hat{T}_{bsl} = \hat{T}(\zeta_m - \Delta\zeta)$, which is integrated to get

$$\hat{v} = \frac{\eta_* \hat{T}_b}{k T_b^{1/2}} \ln \left(\frac{\zeta - \zeta_m}{\zeta_{OB}} \right) + \frac{\eta_*}{k T_b \xi_N} (T_{bsl} - \hat{T}_b) (\zeta - \zeta_m)$$

for

$$\zeta_{bsl} > \zeta > \zeta_m + |\zeta_{OB}|$$

where ζ_{OB} is the nondimensional bottom surface roughness. The velocity at ζ_{bsl} is \hat{v}_{BE} , which serves as a lower boundary condition for the interior Ekman solution.

Velocity in the Ekman layer is found from integrating

$$\frac{\partial \hat{v}}{\partial \zeta} = \frac{1}{K_*} \hat{T}$$

to get

$$\int \hat{v} d\zeta = -i\delta \left[\hat{A} (e^{\hat{\delta}\zeta} + e^{-\hat{\delta}\zeta}) - e^{-\hat{\delta}\zeta} \right]$$

Let

$$\hat{v}_{COR} = \hat{v}_{BE} + i\delta \left(2\hat{A} \cosh \hat{\delta}\zeta_{bsl} - e^{-\hat{\delta}\zeta_{bsl}} \right)$$

so that velocity in the Ekman layer is given by

$$\hat{v}(\zeta) = -i\delta (2\hat{A} \cosh \hat{\delta}\zeta - e^{-\hat{\delta}\zeta}) + \hat{v}_{COR}$$

for

$$-\xi_N > \zeta \geq \zeta_{bsl}$$

For the upper surface ($\zeta > -\xi_N$), the solution, including the log-linear effect if surface buoyancy is present, is given (see McPhee, 1981) by

$$\hat{v} = \hat{v}_{\xi_N} - \frac{\eta_*}{k} \left[\ln \frac{|\zeta|}{\xi_N} - (\hat{\delta} - a)(\zeta + \xi_N) - \frac{a}{2} \hat{\delta} (\zeta^2 - \xi_N^2) \right]$$

for

$$\zeta > -\xi_N$$

where \hat{v}_{ξ_N} is the velocity at the top of the Ekman layer ($\zeta = -\xi_N$) and 'a' is a combination of stability parameters, equal to zero for neutral stability.

When the layer becomes so shallow (in nondimensional coordinates) that the top and bottom surface layers overlap, the maximum extent of each layer is limited to half the depth, and the problem becomes similar to Figure 1, except that slight variation in stress is allowed.

3* Theoretical Results

Figure 4 shows a comparison of stress and mean velocity in boundary layers of four depths. The profiles are presented in coordinates of the nondimensional variables, in order to emphasize that the nondimensional depth in a particular location varies inversely with u^* , which (if the ice cover is thin) is nearly proportional to the surface wind. At a given location, the dynamic depth will be approximately halved by a doubling of the wind speed. The common parameters used in the calculations of Figure 4 were: $u^* = 1$ cm/s, $\omega = 1.3 \times 10^{-4} \text{ s}^{-1}$ (latitude 63 degrees), $z_{OT} = 5$ cm, $z_{OB} = 2$ cm. With these values one can read velocity and stress directly in CGS units. Bottom depths are marked, and it is apparent that $\zeta = 0.5$ corresponds to a dimensional depth of about 38 m.

The upper plot shows a boundary layer with no bottom. Note how both the stress and velocity spiral rightward with increasing depth. The effect of the logarithmic surface layer is apparent in the large shear right near the surface and accounts for the fact that the angle between the stress and the surface velocity is about 22 rather than the 45 required by the straight Ekman solution. As the bottom shoals in the subsequent solutions, we see a more and more significant bottom stress, which according to the reasoning in Section 2, produces a pronounced log layer at the bottom. The orientation of the bottom stress, which controls the direction of enhanced shear in the bottom surface layer, has some interesting consequences for the surface velocity: e.g., when the depth is 20 m, the bottom stress is almost at right angles to the surface stress and the bottom surface layer shear comes mainly in the transverse (imaginary) component of velocity. This gives the surface velocity a much greater deflection than it would otherwise have had. With deeper bathymetry, the bottom shear layer acts to oppose the downwind component, thus the real component of surface velocity is decreased from its deep water value. For depths less than about 20 m, the bottom stress has a downwind component which serves to increase the downwind component of surface velocity, while decreasing the rightward deflection.

Figure 4 suggests that the drag relationship between surface (interracial) stress and surface (ice) velocity may be quite different when the water column is shallow; and this is further demonstrated by Figure 5 where surface velocity and rightward deflection are plotted versus u^* for the four depths. Note that if the ice is thin enough to be ignored in the force balance, the range shown corresponds to winds up to about 40 kt. For a quadratic drag with constant turning,

such as used for the AIDJEX model, V . would be a straight line with slope inversely proportional to the square root of the drag coefficient. The deep water case is fairly well approximated by quadratic drag. For the other depths, the drag law **is** changed by the presence of the bottom. At 10 m, for example, V . is nearly linear over a broad range, but the drag and turning angle are much reduced, essentially because there are two high shear log layers instead of one. At depths of 20 to 40 m, the transition between deep and shallow regimes occurs in the range of winds that would be considered typical, thus these results imply that the drag law needs modification over a good part of the shelf, when the water column is completely mixed.

The above results also hold some interesting implications for ice interaction on the shelf as demonstrated by a thought experiment sketched in Figure 6. We imagine a shelf region that is initially quiescent, but well mixed to the bottom or to 40 m, whichever is shallower. Now suppose that a steady, uniform wind is applied, and that a short time later the turbulent boundary layer is well established, but no slope currents or internal ice forces have had time to build. According to the theory, the surface velocity field should look in plan view like the first row of drift vectors. The outer two vectors, which overlie the **pycnocline** and are therefore cut off from bottom effects, represent the far **field** oceanic boundary layer. Note the appearance of a "jet" in the nearshore region, and differing amounts of offshore ice transport (shown by the dashed components). While this picture is obviously speculative, it shows that the bottom effect could produce by itself considerable shear and a tendency toward convergence or divergence in the ice cover.

To the extent that these ideas apply to a real situation, they also have some novel consequences for oceanic transport; i.e. , the integral of the velocity profile. Since the divergence of this transport is responsible for pressure gradients that give rise to coastal currents, modification as large as that shown by the top row of vectors in Figure 6 may have a significant impact on the details of current set-up, and on storm surge prediction. While these results are far from definitive, they raise some provocative questions.

4. Summary

This work has shown that the rotational effects on the turbulent stress profile in relatively shallow water can have an appreciable, and sometimes surprising, impact on velocity in **the** water column, including the surface (ice) motion. Even in the absence of other coastal effects, shallow bathymetry may cause relatively large shear and divergence in a free-drift ice cover.

The aim here has been to extend a boundary **layer** theory that has successfully described ice/water momentum transfer in other contexts to the nearshore region where the bottom can no longer be ignored. Its application here is restricted to highly idealized conditions and it is best to think of these results as part of a superposition of many effects; nevertheless, **it** seems clear that pure "wind-drift" currents are a major factor in shelf circulation (**Aagaard**, 1981). The obvious need is for more data: not from times when the water is highly stratified (summer), or when the ice is thick and fast; but from the period during freeze-up when the near-shore ice is relatively mobile.

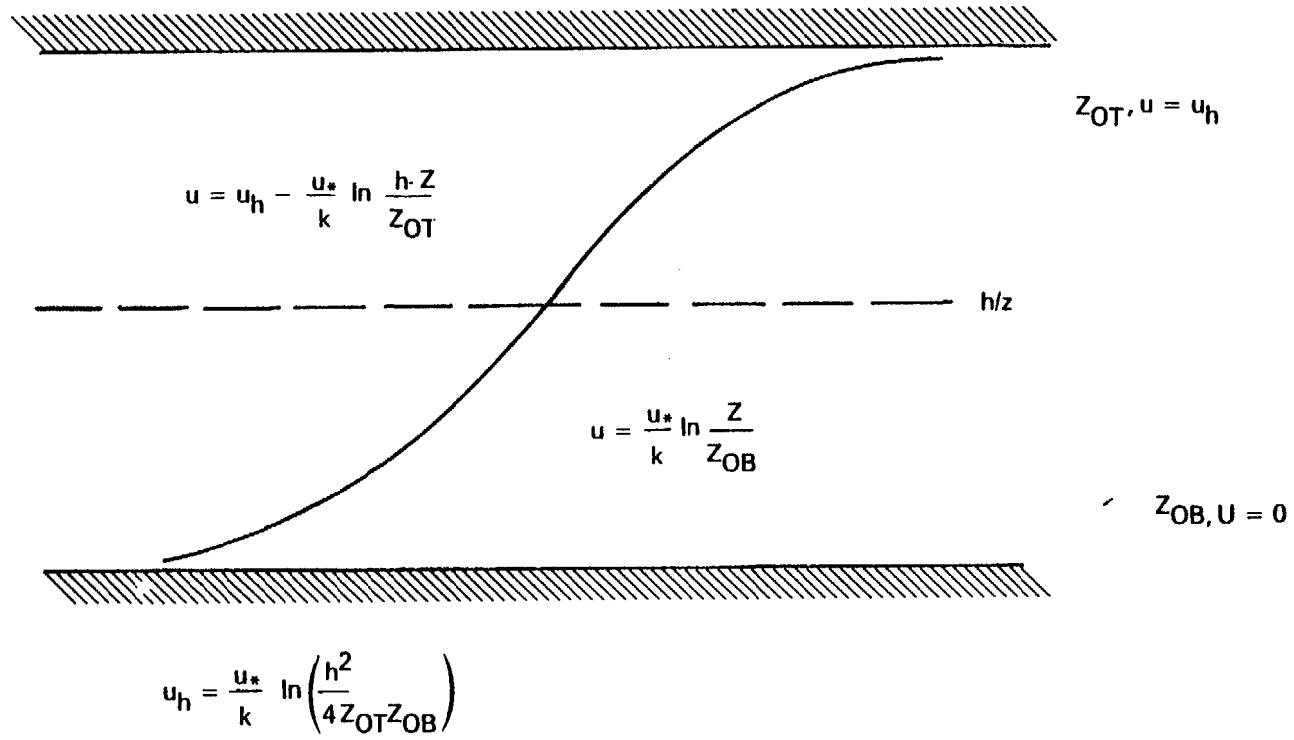
The main question posed here is how the turbulent stress profile evolves from being nearly constant through a shallow water column, to the pronounced rotation seen **in** a deep water **PBL**. In this formulation, the closure technique is to force the stress gradient to zero at the bottom. This is consistent with the physics of rotating flows, although at first glance it seems to contradict the symmetry between upper and lower layers. Consider the elemental force balance:

$$\text{if } \hat{U} = \frac{\partial \hat{\tau}}{\partial z}$$

In words, the gradient of stress is proportional to the component of fluid velocity perpendicular to the stress. Near the surface the angle between mean velocity and stress is at its largest, so the stress gradient **is** most pronounced there. Close to the bottom, the stress and velocity are almost collinear, so it follows that the stress gradient must be quite small. Numerical modeling of the turbulent regime would probably add important insight here -- my feeling is that it would show some details of **the** stress distribution near the bottom to be different from the present model; but that the qualitative conclusions would remain unaltered.

References

- Aagaard, K. (1981) "'Current Measurements in Possible Dispersion Regions of the Beaufort Sea,'* unpublished manuscript, Final Narrative Report, Contract No. 03-5-022-67, **T.O. 3**, University of Washington, Seattle, pp. **74**.
- Garrison, G. R., Welch, M. L. , and **Shaw, J. T.** (1979) "Oceanographic Measurements in the **Chukchi** Sea, April-August 1977,'" Technical Report **APL-UW 7824**, Applied **Physics** Laboratory, University of Washington, Seattle.
- McPhee, M. G. (1981) "An Analytic Similarity Theory for the Planetary Boundary Layer Stabilized by Surface Buoyancy,*' Boundary-Layer Meteorol., **21**, pp. 325-339.



Figure

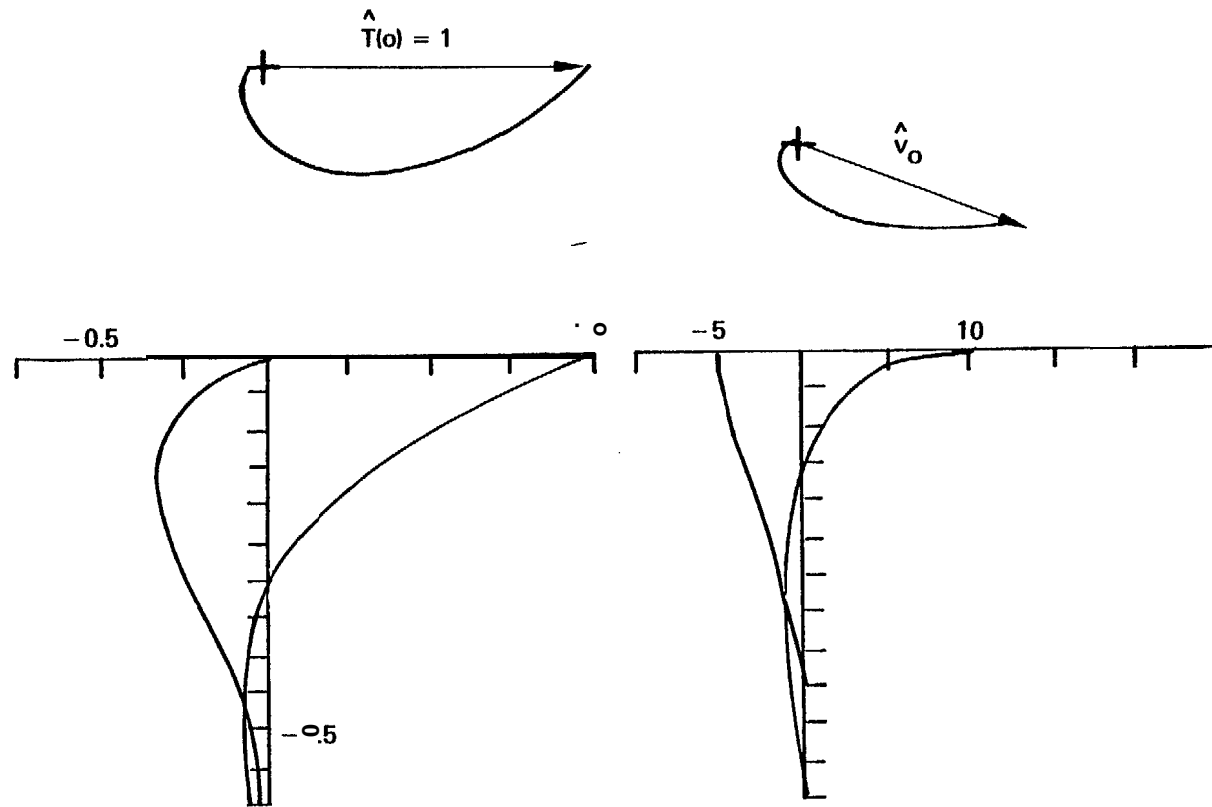


Figure 2.

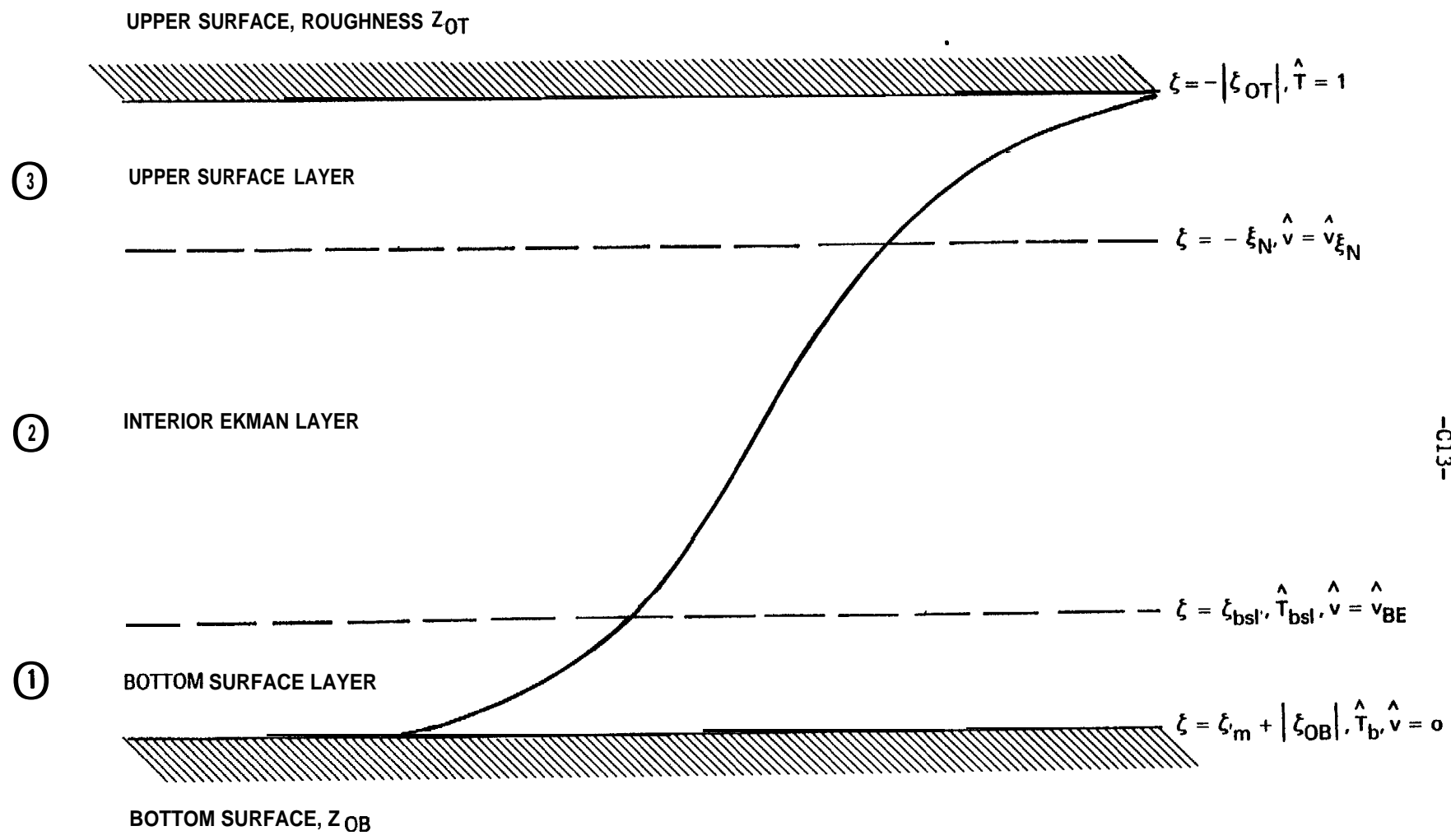


Figure 3.

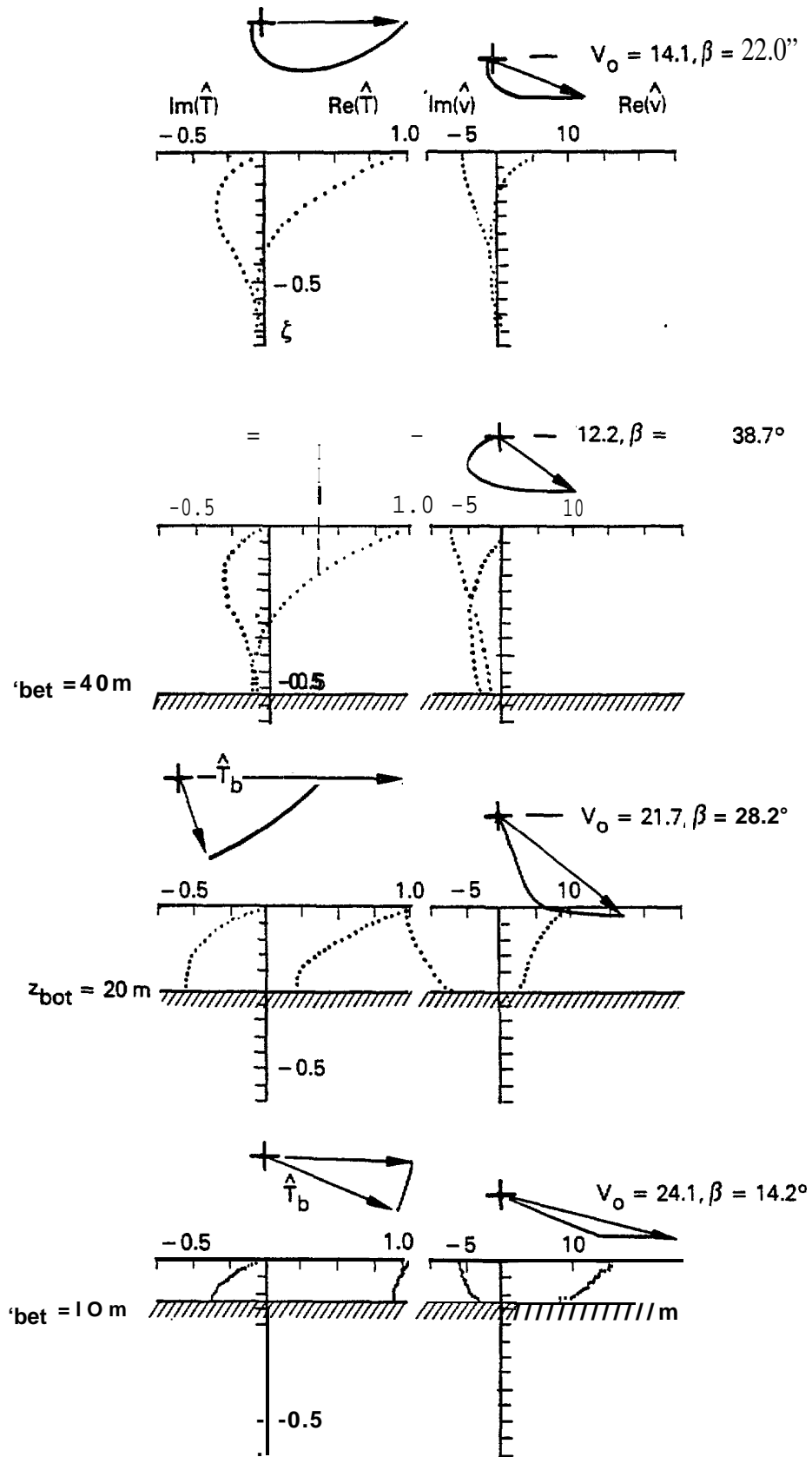


Figure 4,

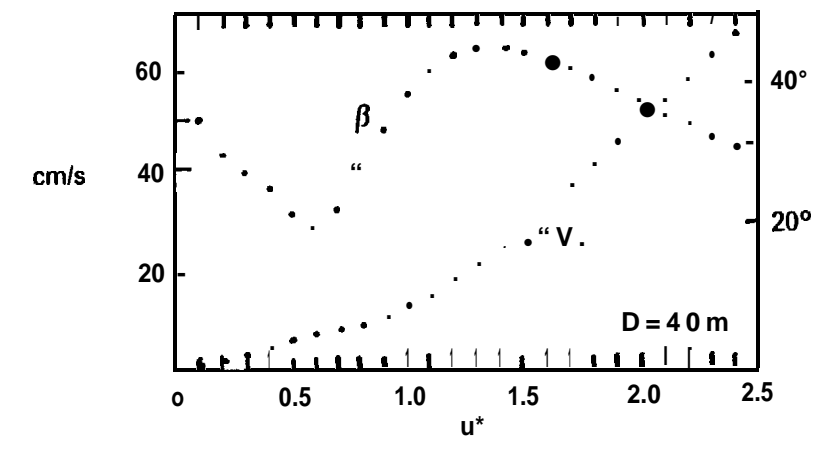
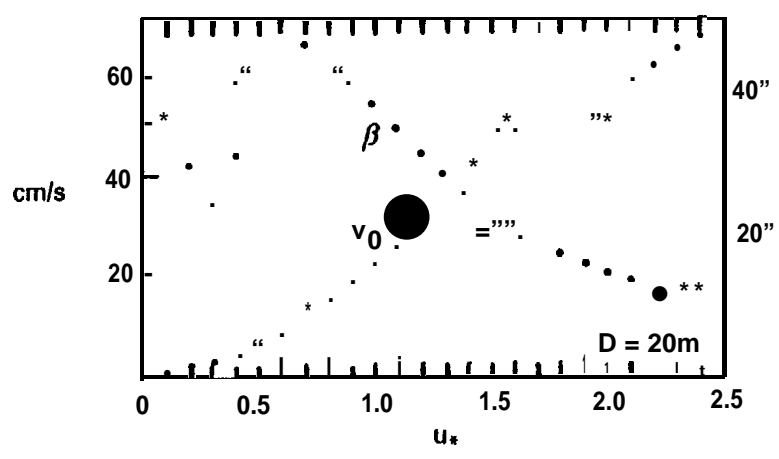
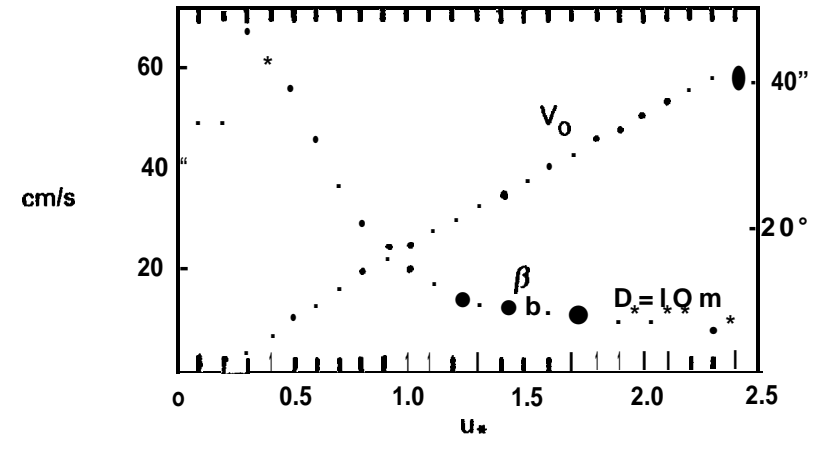
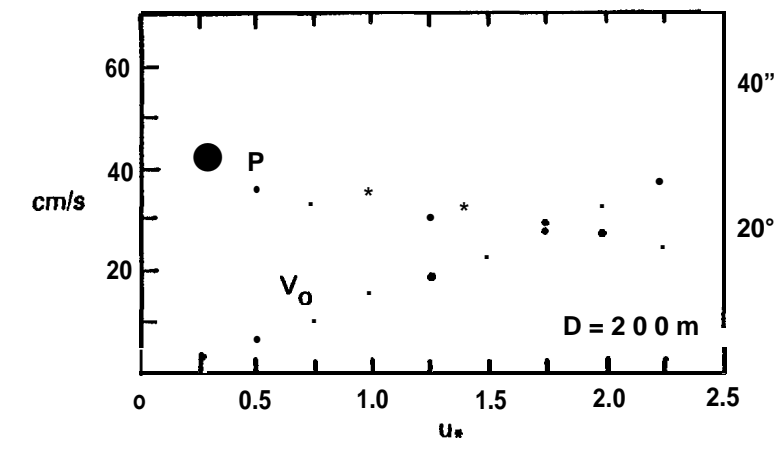


Figure 5.

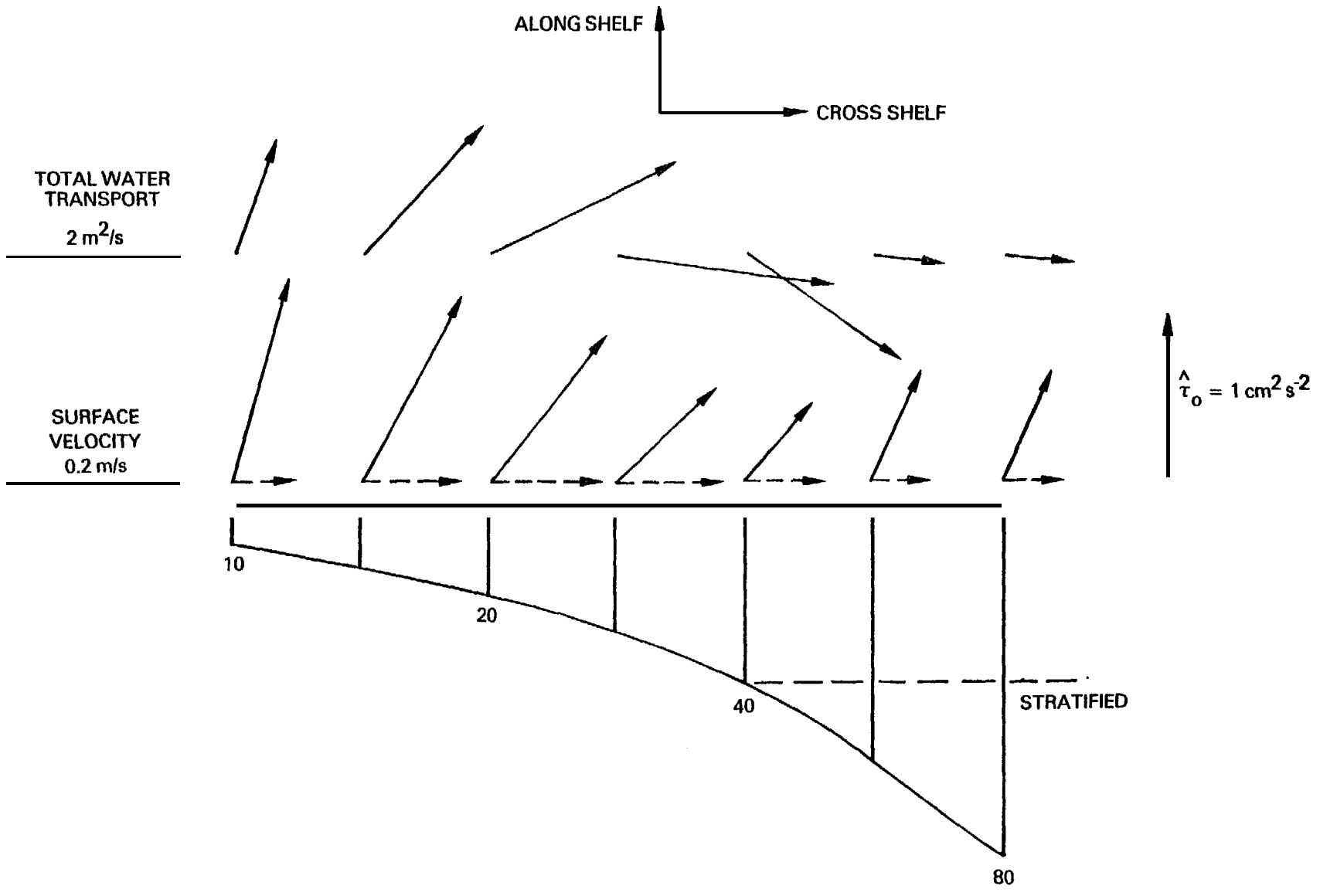


Figure 6.